

1 This paper has undergone peer-review and has been accepted for publication in a special publication of
2 the American Geophysical Union entitled “Noisy Oceans: Monitoring Seismic and Acoustic Signals in
3 the Marine Environment”.
4

5 **Seismic and Acoustic Monitoring of Submarine Landslides: Ongoing Challenges, Recent Successes**
6 **and Future Opportunities**

7 Clare, M.A.^{1*}, Lintern, D.G.², Pope, E.³, Baker, M.³, Ruffell, S.³, Zulkifli, Z.¹, Simmons, S.⁴, Urlaub,
8 M.⁵, Belal, M.¹, Talling, P.J.³

9 1) National Oceanography Centre, Southampton, SO14 3ZH, UK

10 2) Natural Resources Canada, Geological Survey of Canada, Sidney, British Columbia V8L 4B2,
11 Canada

12 3) Departments of Earth Sciences and Geography, University of Durham, Stockton Road, Durham,
13 UK, DH1 3LE, UK

14 4) Earth and Environment Institute, Hull, UK

15 5) GEOMAR Helmholtz Centre for Ocean Research, Kiel, Germany.

16
17 *Contact: m.clare@noc.ac.uk

18
19 **Abstract**

20 Submarine landslides pose a hazard to coastal communities due to the tsunamis they can generate, and
21 can damage critical seafloor infrastructure, such as the network of cables that underpin global data
22 transfer and communications. These mass movements can be orders of magnitude larger than their
23 onshore equivalents and are found on all of the world’s continental margins; from coastal zones to hadal
24 trenches. Despite their prevalence, and importance to society, offshore monitoring studies have been
25 limited by the largely unpredictable occurrence of submarine landslide and the need to cover large
26 regions of extensive continental margins. Recent subsea monitoring has provided new insights into the
27 preconditioning and run-out of submarine landslides using active geophysical techniques, but these tools
28 only measure a very small spatial footprint, and are power and memory intensive, thus limiting long
29 duration monitoring campaigns. Most landslide events therefore remain entirely unrecorded. Here we first
30 show how passive acoustic and seismologic techniques can record acoustic emissions and ground motions
31 created by terrestrial landslides. We then show how this terrestrial-focused research has catalysed
32 advances in the detection and characterisation of submarine landslides, using both onshore and offshore
33 networks of broadband seismometers, hydrophones and geophones. We then discuss some of the new

34 insights into submarine landslide preconditioning, timing, location, velocity and their down-slope
35 evolution that are arising from these advances. We finally outline some of the outstanding challenges, in
36 particular emphasising the need for calibration of seismic and acoustic signals generated by submarine
37 landslides and their run-out. Once confidence can be enhanced in submarine landslide signal detection
38 and interpretation, passive seismic and acoustic sensing has strong potential to enable more complete
39 hazard catalogues to be built, and opens the door to emerging techniques (such as fibre-optic sensing), to
40 fill key, but outstanding, knowledge gaps concerning these important underwater phenomena.

41

42 **1. Introduction**

43 Submarine landslides can be orders of magnitude larger than those on land, occur on remarkably low
44 angle (<2 degree) slopes, and can generate run-out that travels hundreds to thousands of kilometres into
45 the deep-sea (Moore et al., 1989; Hampton et al., 1996; Nisbet and Piper, 1998; Piper et al., 1999; Carter
46 et al., 2014). Underwater slope failures can generate tsunamis that inundate coastal communities that
47 sometimes result in major loss of life (e.g. Harbitz et al., 2014; Tappin et al., 2014), and adversely impact
48 critical seafloor infrastructure networks, such as the cables and pipelines on which we rely for global
49 communications, the Internet, and energy supplies (Piper et al., 1999; Carter et al., 2014). To date, most
50 studies of submarine landslides and their run-out have been based upon analysis of the deposits that past
51 events left behind. These studies have used combinations of: i) seafloor surveys (e.g. multibeam
52 echosounders and side scan sonars) to image submarine landslides in planform (e.g. Prior et al., 1982;
53 McAdoo et al., 2000; Mountjoy et al., 2009; Casas et al., 2016; Normandeau et al., 2019; Brackenridge et
54 al., 2020); ii) sub-surface geophysical surveys to determine the geometry and internal character of
55 submarine landslide deposits (e.g. Gee et al., 2006; Bull et al., 2009; Vardy et al., 2012; Nwoko et al.,
56 2020); iii) intrusive sampling or coring to calibrate geophysical interpretations, provide material for
57 geochronological analysis (age and recurrence determination), and/or determine their source using
58 geochemical and other analytical techniques (e.g. Geist and Parsons, 2010; Dugan, 2012; Urlaub et al.,
59 2013; Vanneste et al., 2014); iv) in-situ or laboratory-based testing to understand geotechnical and
60 geomechanical behaviour of submarine landslides (e.g. Sultan et al., 2010; Ai et al., 2014; Miramontes et
61 al., 2018); v) analysis of ancient, exhumed submarine landslides from rock outcrops (e.g. Brookes et al.,

62 2018; Bull et al., 2019; Ogata et al., 2019) and; vi) physical and numerical modelling to quantify slope
63 stability, post-failure behaviour and resultant impacts (e.g. to seafloor infrastructure or the tsunami that
64 they may initiate) (e.g. Sultan et al., 2010; Harbitz et al., 2014; Tappin et al., 2014; Puzrin et al., 2016).

65

66 These techniques provide valuable insights into the location, extent and nature of past failures, as well as
67 providing the building blocks for generating models that enable inference of the likely behaviour of future
68 events; however, they do not capture the behaviour of field-scale submarine landslides in action and do
69 not reveal the in-situ conditions at the time of failure. Numerical models therefore remain relatively
70 poorly constrained and many key questions remain unanswered; particularly with regards to the initiation,
71 kinematics and impacts of submarine landslides. For instance, what are the preconditioning factors for
72 failure and over what timescales are they important? Why are external triggers (e.g. earthquakes, tropical
73 cyclones) more effective in some settings compared to others? What lag-times may be involved following
74 cumulative or sudden perturbations that precede failure, and what controls that delay? Such information is
75 critical to understand precisely how and when landslides are triggered and develop effective early
76 warning systems, and to understand any climate change feedbacks (e.g. Maslin et al., 2004; Paull et al.,
77 2007; Harbitz et al., 2014; Brothers et al., 2013; Normandeau et al., 2021). Key questions also remain
78 unanswered on the kinematic behaviour of submarine landslides as they propagate. For example, what
79 kinematics are involved during different styles of slope failure and how does that change as the mass
80 travels down-slope? Why do some slopes fail suddenly, with major and rapid displacements, while others
81 move much more slowly and progressively? Does failure type control the nature and extent of run-out,
82 and if so, how? These, and many other, questions remain open, largely due to the challenges involved in
83 monitoring failure processes and their precursor conditions in marine settings, in real time, that often
84 cover very large areas.

85

86 Some of the challenges that inhibit monitoring of submarine landslides include:

- 87 • The *water depths* of many of the settings where submarine landslides occur place financial and
88 logistical constraints on long-duration and continuous monitoring (e.g. Talling et al., 2013; Clare
89 et al., 2017). While slope failures can occur in shallow water deltaic or fjord settings (e.g. Prior et

90 al., 1989; Biscara et al., 2012), many occur in hundreds to thousands of metres water depth and
91 have been documented in the deepest hadal trenches on Earth (Strasser et al., 2013; Kioka et al.,
92 2019).

- 93 • The *remote nature* (i.e. location far from shore) of many submarine landslides provides
94 constraints for power, communications and data transfer. This in turn limits the resolution and
95 frequency of measurements that can be made due to a reliance on in-situ power supplies and
96 recovery and redeployment of instruments by expensive vessels (Urlaub and Villinger, 2019).
- 97 • The *unpredictable nature of submarine landslides over time*. As many studies have suggested that
98 submarine landslide recurrence may be Poissonian (i.e. approximately random), predicting when
99 a specific seafloor slope may fail is a key challenge (Geist and Parsons, 2010; Urgeles and
100 Camerlenghi et al., 2013; Urlaub et al., 2013). While relatively small (e.g. $<1000 \text{ m}^3$) submarine
101 landslides might be relatively frequent (e.g. one or more per year) in high sediment-supply
102 settings (e.g. fjord-head deltas), the events that pose a greater threat to seafloor infrastructure or
103 are tsunamigenic (e.g. $\gg 1 \text{ km}^3$) tend to recur on much longer timescales (e.g. 100s->1000s of
104 years). Continuous observations are required to capture these episodic events.
- 105 • The *large extent of areas affected by slope instability* means that monitoring at point-locations
106 may completely miss events that occur elsewhere along the same margin (McAdoo et al., 2000;
107 Urgeles and Camerlenghi et al., 2013; Casas et al., 2016; Collico et al., 2020; Gamboa et al.,
108 2021). Being in precisely the right place at the right time is highly unlikely in all but a few
109 settings where the controls on slope instability are well constrained (e.g. seasonally-active,
110 spatially-focused sediment supply at steep submarine deltas; Lintern et al., 2016).
- 111 • The *powerful nature of the landslide and its run-out* poses a hazard to monitoring infrastructure
112 that is placed in the way of a landslide (e.g. Inman et al., 1976; Khripounoff et al., 2003). Recent
113 examples of field-based monitoring demonstrate how even relatively small flows can damage and
114 displace sensors and associated equipment (e.g. Inman et al., 1976; Clare et al., 2020 and
115 references therein). Large slope failures would likely completely destroy monitoring arrays in
116 their path.

117

118 **1.1. Recent advances in direct monitoring of submarine landslides**

119 Despite these challenges, recent technological advances have enabled monitoring of several aspects of
120 submarine landslide behaviour. Geotechnical monitoring provides information in relation to the
121 preconditioning of submarine landslides, through use of in-situ devices that monitor changes in
122 subsurface conditions, such as pore pressure (e.g. Prior et al., 1989; Strout and Tjelta, 2005; Stegmann et
123 al. 2011). Technological advances have triggered a recent growth in geophysical monitoring of aspects of
124 submarine landslides including: i) repeated seafloor surveys (at timescales from decades to minutes in
125 some cases) to document elevation changes, evolution of the landslide itself, the effects of landslide run-
126 out on the seascape, and subsequent reworking by other marine processes (e.g. Smith et al., 2007; Biscara
127 et al., 2012; Kelner et al., 2016; Mastbergen et al., 2016; Fujiwara et al., 2017; Chaytor et al., 2020;
128 Heijnen et al., 2020; Guiastrennec-Faugas et al., 2021; Normandeau et al., 2021); ii) time-lapse reflection
129 seismic surveys to monitor changes in subsurface conditions (e.g. Blum et al., 2010; Hunt et al., 2021;
130 Roche et al., 2021; Waage et al., 2021); (iii) direct monitoring of turbidity currents (some of which likely
131 initiated from submarine landslides) using moored or vessel-based, active acoustic sensors, such as
132 Acoustic Doppler Current Profilers (ADCPs) and multibeam sonars, that enable measurement of flow
133 velocity and estimation of suspended sediment concentrations (e.g. Xu et al., 2010, 2011; Hughes Clarke
134 et al., 2012; Khripounoff et al., 2012; Simmons et al., 2020); and iv) monitoring changes in seafloor
135 movement and elevation via geodetic location of acoustic transponders (e.g. Campbell et al., 2015; Paull
136 et al., 2018; Urlaub et al., 2018; Zhao et al., 2021). Such studies tend to involve either campaign-style
137 surveys (often with years between individual campaigns), short duration (i.e. weeks to months-long)
138 continuous measurements (as they are limited by power supply and data storage), or else require cabled
139 connection for data transfer and external power supply. Therefore, while they provide detailed (i.e.
140 temporally or depth/laterally-resolved) measurements, such approaches necessarily cover short time
141 periods and limited areas relative to the full extent of continental slopes that may be affected by slope
142 instability, as well as the extent of an individual landslide event itself (Urgeles and Camerlenghi et al.,
143 2013; Urlaub and Villinger, 2019; Brackenridge et al., 2020; Fan et al., 2020). These studies also
144 primarily focus on slope preconditioning, or the run-out produced by slope failures; hence, significant

145 knowledge gaps remain with regards to the inception of slope failures, their kinematics, and their
146 transition from slope failure to more dilute run-out, which are key, but poorly constrained parameters in
147 tsunami modelling, impact assessments for critical seafloor infrastructure, and in understanding deep
148 water sediment transport in general.

149

150 **1.2. Aims**

151 There is thus a compelling need for low power-consumption sensors that can cover large spatial domains,
152 which are capable of monitoring a wide range of environmental conditions (including the timing, location
153 and behaviour of submarine landslides), and for systems that are deployed offshore to generate
154 sufficiently small data volumes, such that sustained, long-endurance, autonomous monitoring is possible.

155 Here, we show how passive acoustic and seismological monitoring has started to address these constraints
156 and can contribute to filling key knowledge gaps. First, we explore the application of passive acoustic and
157 seismological monitoring of terrestrial landslides, and the relevance of those techniques in the marine
158 realm. Second, we discuss which aspects of submarine landslides may be detected using passive acoustic
159 and seismological monitoring. Here, we explore the kinds of environmental noise or ground motion that
160 are generated by submarine landslides, and therefore what signals we should anticipate recording. Third,
161 we present examples from recent marine studies that have successfully monitored precursor conditions,
162 initiation, movement and impacts of submarine landslides using passive acoustic and seismological
163 approaches. Finally, we conclude with some of the on-going technological developments, and the future
164 application of other techniques, including those detailed in other chapters of this volume.

165

166 **2. Passive geophysical monitoring of terrestrial landslides**

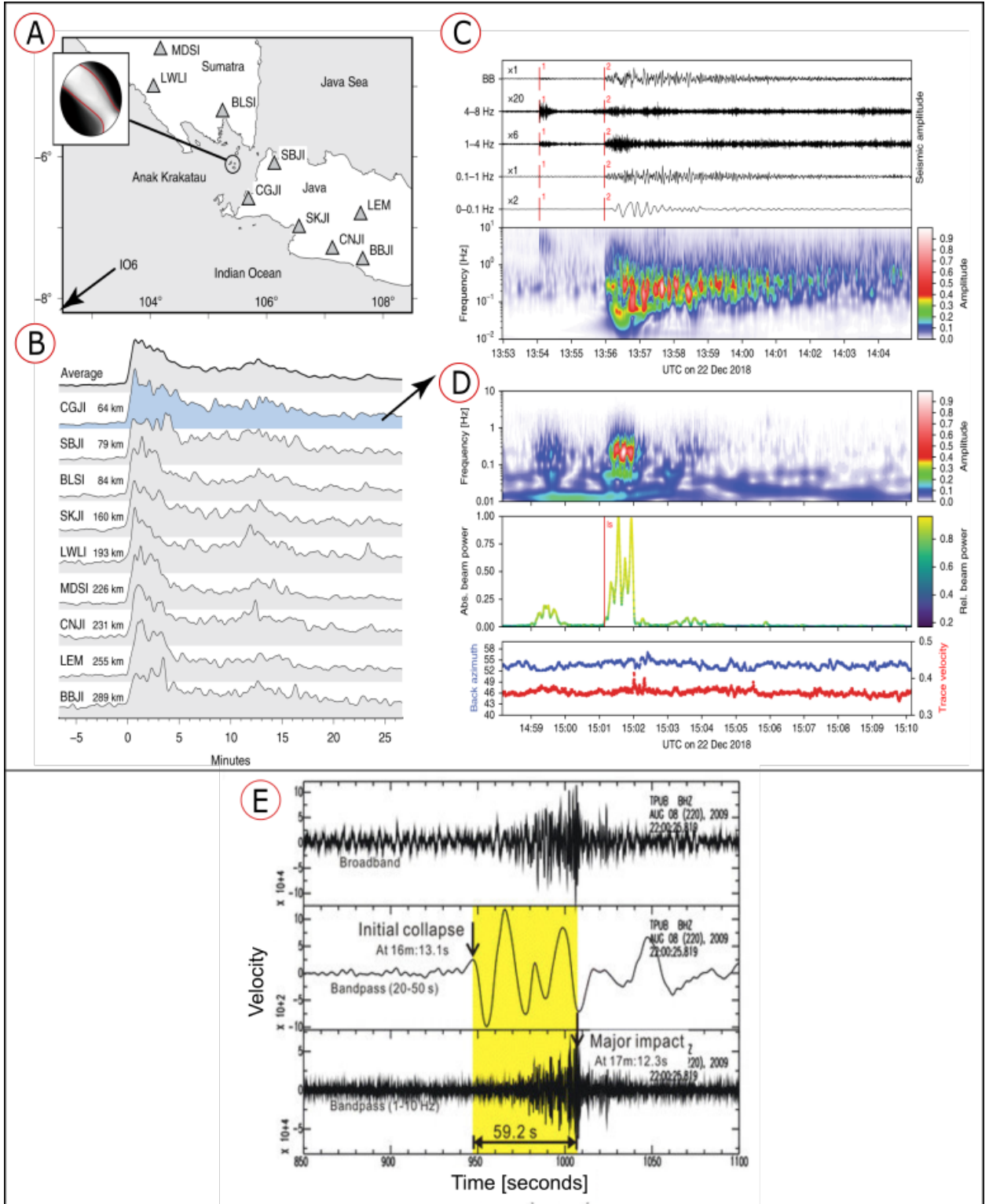
167 Early terrestrial studies successfully identified subsurface mining blasts and earthquakes using
168 seismometers, which stimulated further research into the potential of passive geophysical monitoring to
169 detect onshore slope failures (Galitzin, 1915; Jeffreys, 1923; Antsyferov, 1959; Cadman and Goodman,
170 1967). The elastic straining of soils and rock, friction due to displacement along a failure plane, within the
171 sliding mass, and collision of the landslide mass at its down-slope limit were subsequently recognised as
172 signals that could be recorded by seismologic monitoring techniques (e.g. Cadman and Goodman, 1967).

173 It is now well known that progressive failure and detachment of unstable masses can generate local
174 ground motions that are equivalent to earthquakes; hence, land-based seismological networks are
175 increasingly used to determine the timing and location of slope failures, particularly in remote settings
176 where repeat topographic surveys are rare or non-existent (e.g. Hibert et al., 2019). Such studies enable
177 identification of many landslides that would otherwise be missing from historical records, thus providing
178 significant improvements in the completeness of hazard catalogues (Ianucci et al., 2020).

179

180 In addition to creating ground motions, terrestrial landslide activity can also generate acoustic emissions,
181 most of which tend to have a frequency content similar to, or just below, the spectrum of audible sound
182 (Chichibu et al. 1989; Rouse et al. 1991; Dixon and Spriggs, 2007; Dixon et al., 2015). Acoustic
183 emissions are generated as a slope is subjected to stress, shear and/or the landslide mass starts to move
184 downslope (Dixon et al., 2015); hence, both acoustic emission and seismological monitoring have started
185 to gain recognition as an onshore early warning tool to identify the early stages or precursors to slope
186 failure (e.g. Mainsant et al., 2012; Dixon et al., 2015; Michlmayr et al., 2017; Le Breton et al., 2021).
187 Analysis following the Anak Krakatau volcanic sector collapse in Indonesia (which generated a
188 devastating tsunami in December 2018) revealed that broadband seismic and infrasound monitoring
189 networks detected not only the landslide event, but also potential triggering events that preceded the
190 collapse (Walter et al., 2019; Figure 1). Regional tsunami monitoring networks did not detect the resultant
191 surface wave due to its localised point source, as they were designed to detect longer line sources (Ye et
192 al., 2020). The collapse itself was represented by a short-lived (one to two-minute-long) low frequency
193 (0.01-0.03 Hz) signal; the first P-wave of which was detected at nine onshore seismometers across the
194 Sumatra and Java region, pin-pointing its location at Anak Krakatau (Walter et al., 2019; Figure 1). This
195 event had a moment magnitude (M_w) equivalent to 5.3. A higher frequency (0.1-4 Hz) seismic event was
196 recorded 115 seconds prior to the sector collapse, while the collapse signal was followed by five minutes
197 of a continuous tremor-like signal at high frequencies (0.7-4 Hz) that was attributed to post-failure
198 eruptive activity. Infrasound arrays as far afield as Australia (>1000 km to the south-west) recorded a
199 high-energy impulse that matched the origin times of the short-period seismic signal corresponding to the
200 collapse event (Walter et al., 2019). This example is particularly pertinent, not only because it

201 demonstrates the capability of passive seismological and acoustic monitoring to detect terrestrial
 202 landslides onshore, but also because approximately half of the failed mass was actually under water (Hunt
 203 et al., 2021).



204

205 **Figure 1: Seismic and infrasound records of the 2018 Anak Krakatau volcanic island collapse from**
206 **Walter et al. (2019), including: A) location of regional seismic monitoring network; B) vertical**
207 **component of 0.4-1Hz seismic records at various stations; C) Normalised seismic amplitudes at the**
208 **station nearest to Anak Krakatau recording a high frequency event prior to the collapse (1) and a**
209 **low frequency signal that is related to the landslide (2); D) infrasonic spectrogram records of**
210 **frequency, beam power and back azimuth used to locate the event from a seven-element infrasound**
211 **array. E) Broadband seismogram (above), and band pass filtered by 20-50 seconds (middle) and 1-**
212 **10 Hz as recorded before, during and after the 2009 Hsiaolin onshore landslide in Taiwan by Lin**
213 **(2015). See online version for colour figure.**

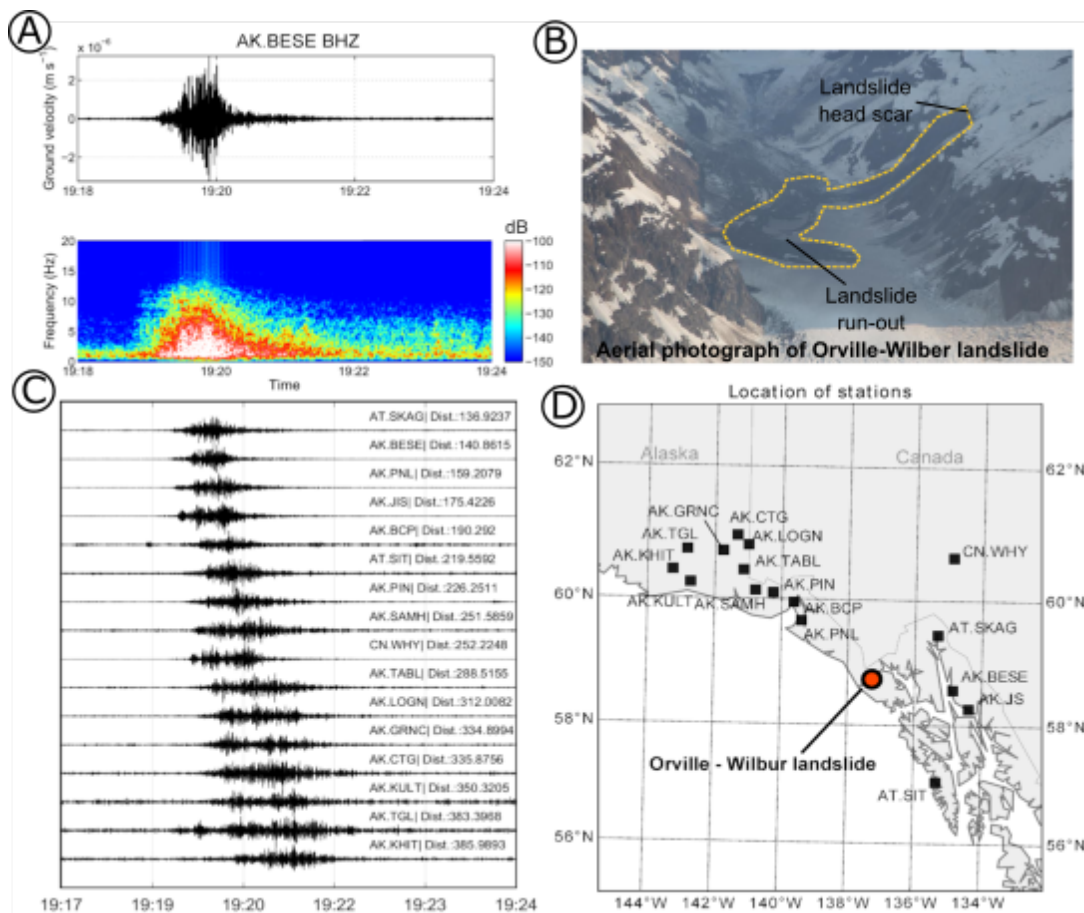
214

215 Onshore seismologic networks have been used to detect terrestrial landslides, including the Hsiaolin
216 hillslope landslide, which occurred when Typhoon Morakot hit Taiwan in 2009. Broadband seismic data
217 recorded: i) very long period seismic signals (20-50 seconds) that were interpreted to be related to elastic
218 rebound of exposed stratigraphy as the overlying landslide mass was evacuated and moved downslope;
219 and ii) large amplitude high frequency signals (1-10 Hz) that were interpreted to result from the impact of
220 the landslide mass at the base of slope (Lin, 2015). Based on the time between these seismic events and
221 the documented run out distance of 2,500 m, Lin (2015) estimated a maximum velocity of >80 m/s. A
222 total of 51 other landslides were also detected on the same day by the same broadband network (Lin et al.,
223 2010). Perhaps most remarkably, 14 of these were detected offshore. Hence, in instances where
224 broadband seismic networks are sufficiently dense, they can provide a useful tool for hazard monitoring.

225

226 Processes that generate ground motion and create collisions within similar gravity-driven mass
227 movements have also been successfully recorded using various passive geophysical techniques,
228 including: i) submerged hydrophones and microphones to measure bedload transport based on noise
229 generated by impacts caused by granular material in rivers and streams (Downs et al., 2016; Geay et al.,
230 2017; Rickenmann, 2017; Geay et al., 2020); ii) bespoke geophone and infrasound arrays that detect self-
231 generated noise and vibrations related to snow avalanches (Suriñach et al., 2005; Besson et al., 2007;
232 van Herwijnen and Schweizer, 2011; Lacroix et al., 2012; Van Herwijnen et al., 2016); and iii) use of

233 existing seismological stations to detect ice avalanches, rock falls and glacial outburst floods from sudden
 234 ground movements as the mass impacts the ground (Caplan-Auerbach and Hugel, 2007; Deparis et al.,
 235 2008; Cook et al., 2018, 2021). The successful demonstration of passive geophysical tools to monitor
 236 terrestrial mass movements has opened the door for the application of similar techniques in offshore
 237 settings, with a view to overcoming some of the many shortcomings of active source monitoring tools
 238 (e.g. particularly in relation to power and spatial limitations). Resolution and signal-to-noise ratio are
 239 often orders of magnitude poorer for submerged instruments, as a result of: i) poor coupling with the
 240 seafloor arising from their crude placement (i.e. where instrument frames are dropped from a ship, as
 241 compared to the precise placement of instruments onshore; and ii) the environmental noise of the water
 242 column, which is affected by a variety of natural processes and human activities.



243

244 **Figure 2: Example of seismic records of terrestrial landslide, from Hibert et al. (2019), which was**

245 **detected by 17 stations between 136 and 385 km from the event itself. A) Seismic signal filtered**

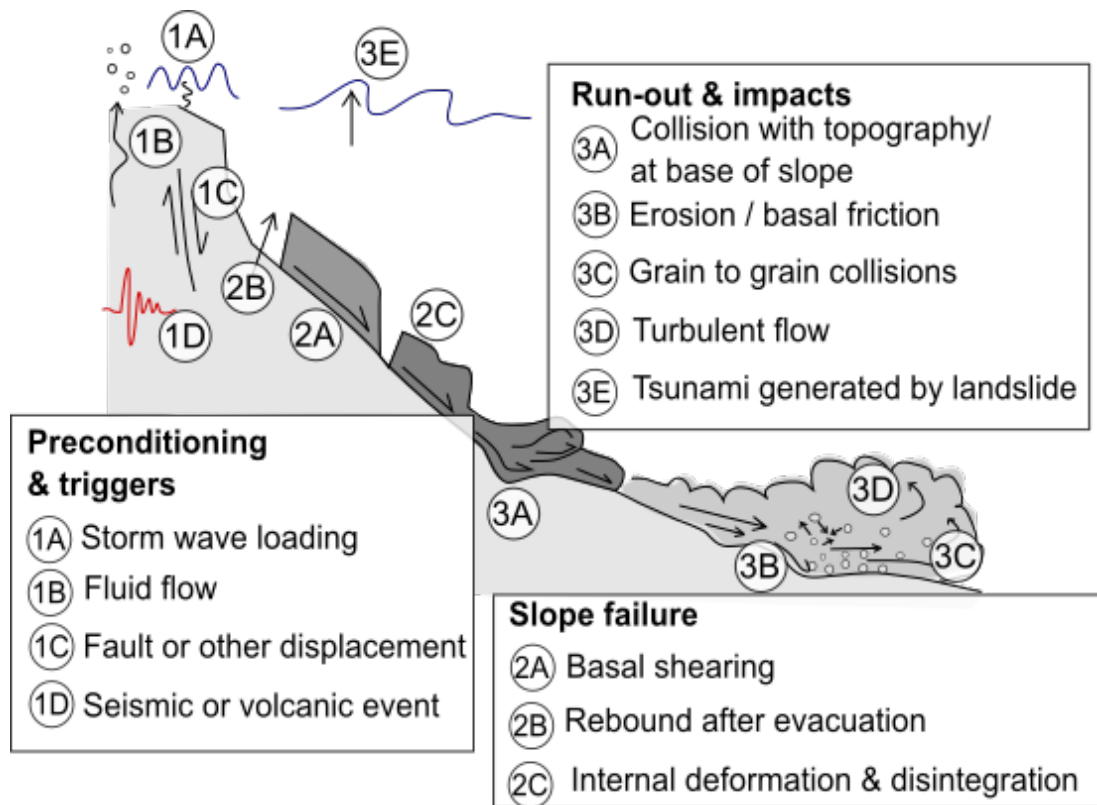
246 **between 1 and 10 Hz. B) Aerial photograph of the landslide which provided the validation of the**

247 **signal interpretation. C) Seismic signals related to the same landslide at 16 locations, which are**
248 **shown in D) in relation to the landslide location. See online version for colour figure.**

249 **3. Which aspects of submarine landslides should we be able to detect with passive systems?**

250 Based on these past studies, a range of information can theoretically be recorded from submarine
251 landslides by passive seismic and acoustic monitoring (Figure 3). We now discuss some of these aspects,
252 broadly in the order in which they would occur (i.e. prior to, during and then following a slope failure).
253 First, data can be acquired in the build up to a slope failure, providing information on preconditioning,
254 including temporal variations in volcanic or subsurface fluid flow activity, as well as potentially
255 identifying any plausible external triggers such as earthquakes, tropical cyclones, storms or rapid
256 sediment delivery by floods. Next, the timing and location of failure can potentially be ascertained by
257 triangulating seismic signals (e.g. the case of the Anak Krakatau event), as a result of ground motions
258 and/or noise generated as shearing occurs along the basal failure surface (and potentially also along its
259 lateral margins), and as that shear propagates through the subsurface (Puzrin et al., 2016). As the
260 landslide mass becomes mobile, ground motions and noise will likely be generated by friction created
261 along the failure plane (Campbell et al., 1995; Brodsky et al., 2003; Gee et al., 2005), due to internal
262 deformation of the moving sediment mass (e.g. Mountjoy et al., 2009; Buss et al., 2019; Sammartini et
263 al., 2021), and if the mass starts to disintegrate as it entrains and mixes with ambient seawater (e.g.
264 Masson et al., 2006). A reduction in vertical effective stress caused by evacuation of overlying sediments,
265 or temporary loading and unloading as a result of the transit of an overriding landslide mass can trigger
266 elastic rebound, producing long period signals (Kanamori and Given, 1982; Kawakatsu, 1989; Lin, 2015)
267 that may occur suddenly, or steadily over prolonged timescales (e.g. >months in onshore examples; Lin,
268 2015; Leung and Ng, 2016). The displaced mass that moves downslope may travel considerable distances
269 (tens to hundreds of km), over relatively low angle (<1-2 degrees) slopes. The ground motions and noise
270 generated will depend on the changing rheology and kinematics of that moving mass, and its interactions
271 with the seafloor and any topography with which it encounters (e.g. Mountjoy et al., 2018). Friction
272 arising from displacement and erosion at the base of the moving mass should be detectable, however the
273 nature of the seafloor substrate may enhance or attenuate any signals that are generated. As the landslide

274 disintegrates, it may switch from a plastically deforming mass of sediment, to a dense slurry dominated
 275 by grain to grain collisions, or a more dilute flow that is characterized by sediment suspended primarily
 276 by turbulence (e.g. Talling et al., 2007; Sumner and Paull, 2014; Paull et al., 2018). Each of these modes
 277 will likely generate different signals. Where the moving mass generates a sudden physical impact and
 278 comes to rest, such as at breaks in slope (ten Brink et al., 2006), following a sudden height drop
 279 (Moernaut and De Batist, 2011), or where it meets pronounced topographic barriers (Frey-Martínez et al.,
 280 2006), strong, high frequency signals should be anticipated (Caplan-Auerbach and Hugel, 2007; Deparis
 281 et al., 2008). Finally, the indirect effects of the landslide may also generate a seismic signal, such as
 282 where displacement of the overlying water mass generates a tsunami (e.g. Yuan et al., 2005).
 283



284
 285 **Figure 3: Schematic illustration of some aspects of submarine landslides capable of generating**
 286 **seismic and/or acoustic noise as discussed in this chapter, relating to preconditioning and triggering**
 287 **(1A-D), landslide inception and down-slope displacement (2A-C) and its subsequent evolution and**
 288 **impacts (3A-E). See online version for colour figure.**
 289

290 **4. Recent advances and opportunities in passive monitoring of submarine landslides**

291 Motivated by successful terrestrial landslide monitoring, and enabled by advances in offshore geophysical
292 monitoring (as highlighted by the other chapters in this volume and Baumgartner et al. 2018), several
293 recent studies have demonstrated that passive monitoring of several aspects of submarine landslides is no
294 longer just a possibility, but a tangible reality. Many challenges remain; most notably the fingerprinting
295 of seismic and acoustic signals. The paucity of direct submarine landslide monitoring studies (for reasons
296 discussed earlier in this chapter) means that many of these signals remain poorly calibrated; hence,
297 understanding the precise cause and source of signals is often unclear. That being said, recent studies
298 have provided important forward steps in understanding previously unresolved aspects of submarine
299 landslides and provide opportunities to fill other outstanding knowledge gaps. We now highlight studies
300 that illuminate three of these areas: i) timing and location; ii) kinematics; and iii) run-out.

301

302 **4.1. Determining the timing and location of submarine landslides at a margin scale using land-**
303 **based seismological networks**

304 Using networks of land-based seismological monitoring stations, seismic sources that did not correspond
305 to catalogued earthquakes or storms have been located from radiating surface waves sourced in the Gulf
306 of Mexico and the South China Sea. In the case of the Gulf of Mexico, 85 such non-earthquake seismic
307 signals were identified between 2008 and 2015, located in various locations on the offshore continental
308 slope, and have been attributed to submarine landslide activity (Fan et al., 2020; Figure 4). Individual
309 landslide locations have previously been proposed from analysis of onshore seismological monitoring
310 (e.g. Dewey & Dellinger, 2008; Ten Brink et al., 2008), but this is the first study to identify multiple
311 submarine landslides. The seismic energy recorded is presumed to have arisen from the fast downslope
312 movement of relatively rigid landslide masses (Fan et al., 2020). Given the density of offshore oil and gas
313 infrastructure in the Gulf of Mexico (which is known to be vulnerable to damage by submarine landslides
314 and their run-out), this study provides a much-improved understanding of the locations that are prone to
315 slope failure (Chaytor et al., 2020). As well as identifying a number of seismic signals attributed to
316 terrestrial landslides from an onshore broadband seismometer network, Lin (2015) also interpreted
317 arrivals from offshore-generated ground motions in a region offshore SW Taiwan, to relate to submarine

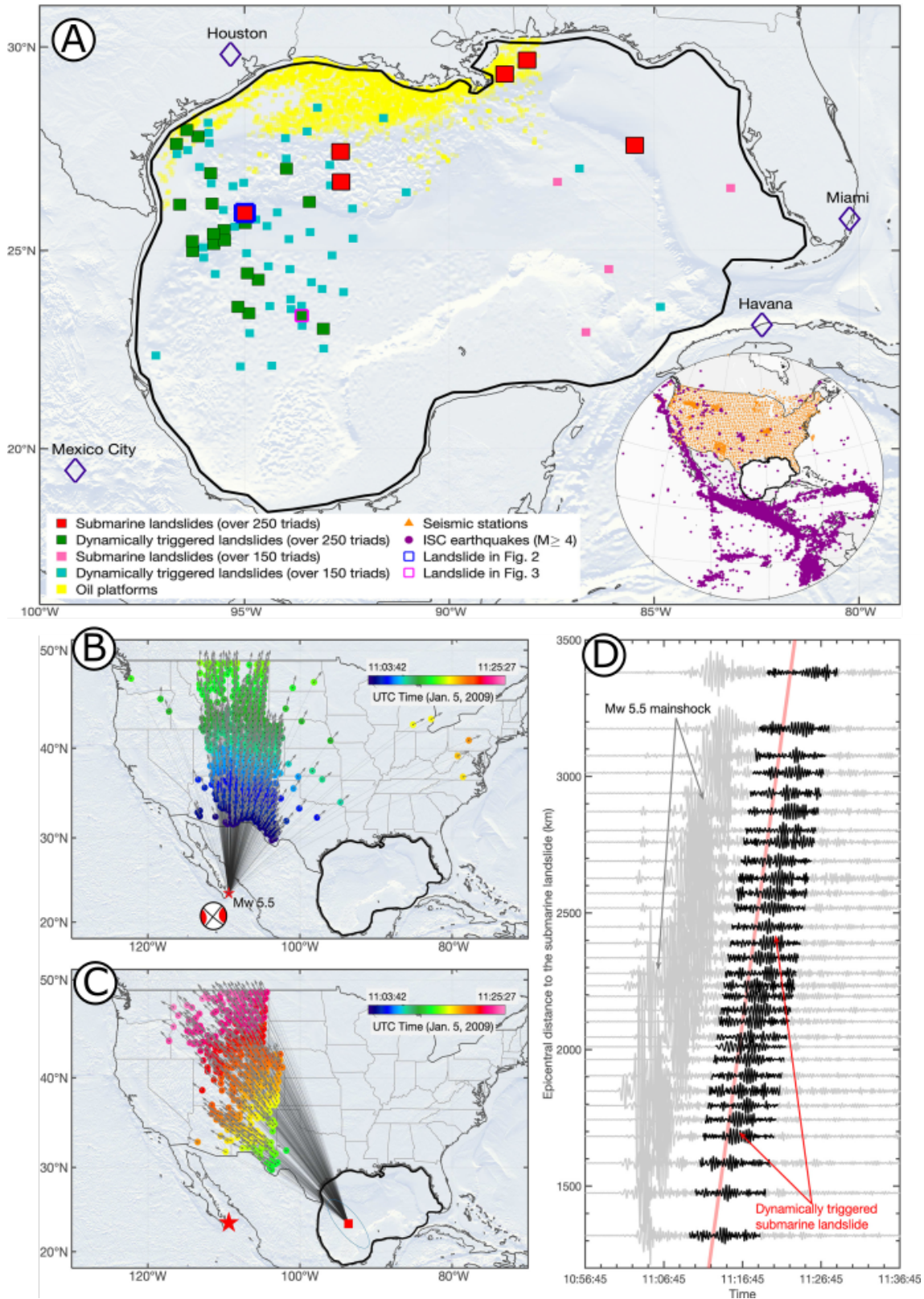
318 landslides, occurring shortly after the passage of the powerful Typhoon Morakot (8th August 2009). The
319 triangulated location of these seismic sources was found to be clustered around submarine canyon flanks
320 and steep continental slopes, which are known to be more prone to slope instability from previous
321 seafloor surveys (Yeh et al., 2021). Submarine sediment flows, that were likely triggered by slope failures
322 and related to this event, damaged a number of telecommunications cables that crossed the Gaoping
323 Canyon (Carter et al., 2014; Pope et al., 2017).

324

325 The ability to identify the timing and location of submarine landslides using existing onshore
326 seismological networks (i.e. without the need for deployment of bespoke underwater sensors) offers a
327 potentially game-changing opportunity to fill gaps in hazard catalogues that are required for the robust
328 and resilient design of offshore engineering projects (e.g. oil and gas, renewables, subsea cables) and for
329 developing hazard assessments for coastal communities (e.g. to inform tsunami warning and guide any
330 related civil response planning). There is still a need to calibrate these interpretations through follow up
331 seafloor surveys to document the true efficacy of the method and determine which landslide types are
332 reliably detected. Indeed, Fan et al. (2020) point out that this approach will likely only detect landslides
333 that generate sufficient seismic energy; hence, slow (e.g. creep-like) or small landslides are unlikely to be
334 detected. While submarine landslide catalogues may become more extensive using this method, they will
335 remain incomplete for such events that do not generate discernable seismic noise. Given the fact that
336 tsunamigenic landslides tend to be faster and larger, this method therefore provides a very promising step
337 forward in submarine landslide detection across very large areas, and will only be strengthened as
338 broadband seismic networks are expanded. A further positive is that these passive detection methods
339 provide a low cost approach to tackle the current biases in submarine landslide studies, given that the
340 majority of these presently focus on the North Atlantic and offshore from more economically developed
341 countries (Clare et al., 2019).

342

343



344

345 **Figure 4: Identification of submarine landslides using terrestrial seismometer networks from Fan**
 346 **et al. (2020). A) Locations of seismic signals interpreted to relate to submarine landslides in the**
 347 **Gulf of Mexico using the onshore seismic monitoring network. Inset shows earthquakes in the**

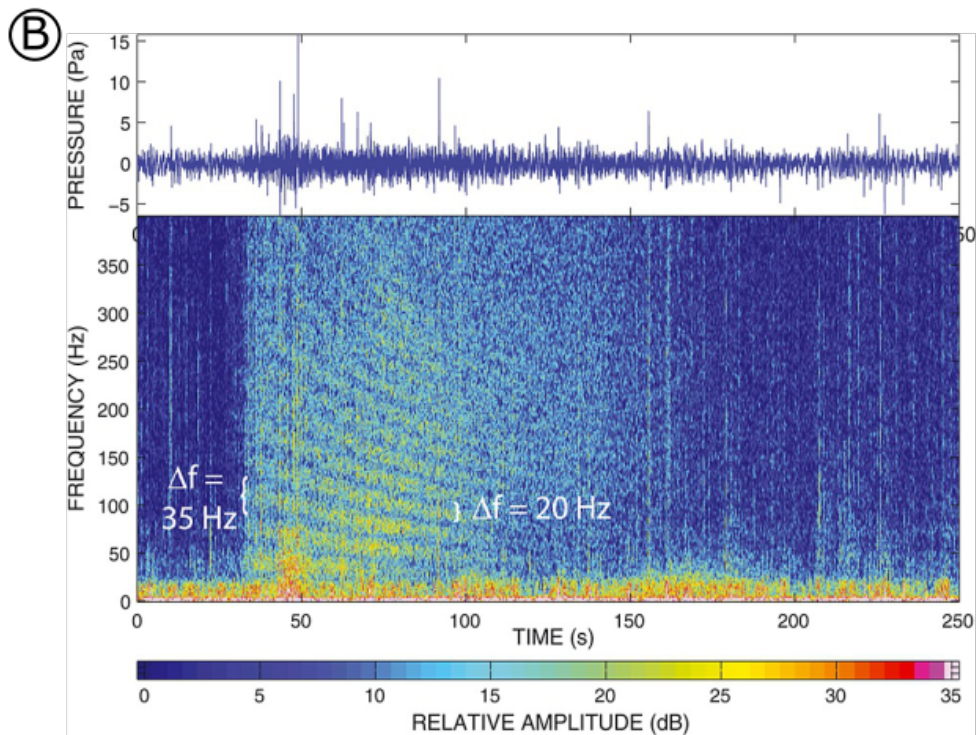
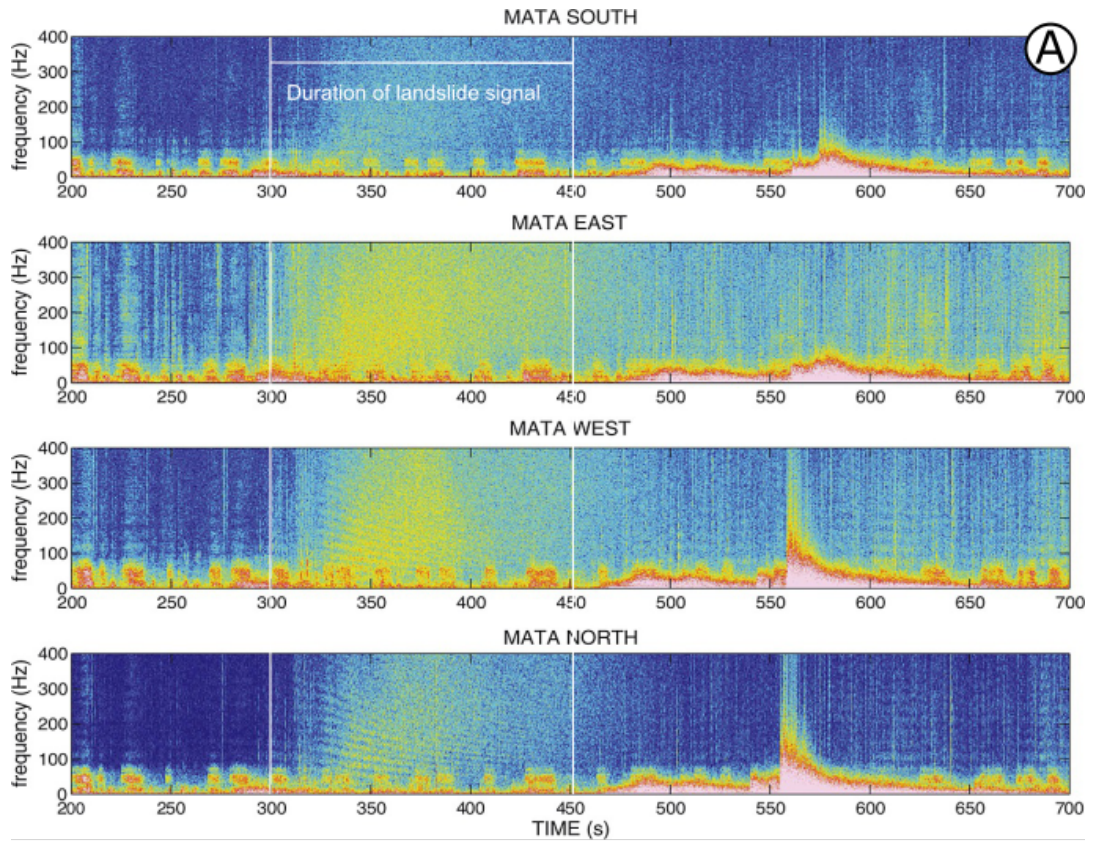
348 **monitored time period (2008-2015) of magnitude 4 or above. B) Rayleigh wave arrival times**
349 **(colours of circles) and propagation directions (lines) for an earthquake, and C) a submarine**
350 **landslide that is thought to have been triggered by that same earthquake (red star). D) Bandpass**
351 **filtered (20-50 seconds) waveforms for a selection of the seismic stations used to locate the**
352 **submarine landslide. Grey signals show precursor earthquake and black shows the signal of the**
353 **landslide itself. See online version for colour figure.**

354

355 **4.2. Quantifying landslide kinematics using hydrophones**

356 Submarine landslide-generated noise has been used to determine the existence of events in remote
357 oceanic settings that would otherwise have likely gone unnoticed. Networks of hydrophones, including
358 the Hawaii Undersea Geo-Observatory in the Pacific Ocean, recorded a combination of partly-subaerial
359 and fully-submarine landslides on the flanks of volcanic islands, which generated acoustic signals that
360 were recorded up to 7000 km from their source; sometimes exceeding the amplitudes generated by
361 volcanic eruptions by up to an order of magnitude (Caplan-Auerbach et al., 2001; Chadwick et al., 2012;
362 Caplan-Auerbach et al., 2014; Figure 5). The distinctive, extremely low frequency signals recorded are
363 thought to relate to the collapse of large landslide blocks, composed of highly competent volcanic
364 material, as well as from their disintegration as they travelled downslope as an avalanche (Chadwick et
365 al., 2012). In these instances, the triggering event generally seems to relate to enhanced volcanic activity,
366 such as at the West Mata volcano near Tonga, and at Kilauea volcano, Hawaii (Caplan-Auerbach et al.,
367 2001; 2014). In addition to pinpointing their location, and identifying the timing relative to volcanic
368 activity, the multi-pathing of the propagated sound waves enabled determination of the landslide transit
369 velocities, which are estimated at between 10 and 25 m/s (Caplan-Auerbach et al., 2014). The location (in
370 particular the water depth) of a landslide source, and its initial velocity, are key inputs for tsunami
371 modelling (e.g. Løvholt et al., 2015). Typically, these parameters remain poorly or entirely un-
372 constrained, which results in a wide uncertainty in any predictive tsunami modelling. Therefore, these and
373 future observations using similar hydrophone networks can play an important role in improving our
374 understanding of a globally significant hazard (e.g. Tappin et al., 2008; Harbitz et al., 2014; Goff and
375 Terry, 2016). Again, calibration of the hydrophone signals is needed; hence, field studies that make multi-

376 parameter measurements of submarine landslide activity will contribute significantly to the fingerprinting
377 of different acoustic responses, and will enhance confidence in the future acoustic detection and
378 characterization of submarine landslides.
379



380

381 **Figure 5: Hydrophone spectrograms showing evidence of submarine landslides in the SW Pacific**
382 **from Caplan-Auerbach et al. (2014). A) The signal between 300 and 450 seconds is interpreted as a**
383 **submarine landslide due to its broadband spectrum and variable frequency content. It is distinct**
384 **from degassing explosions (low frequency, <50 Hz) events and regional earthquakes (very low**
385 **frequency between 470 and 600 seconds). B) Hydrophone time series and spectrogram for a**
386 **submarine landslide. Interference bands are noted – at 35 Hz at the start of the landslide and 20 Hz**
387 **near the end. The change in spacing of frequency bands indicates a moving source and is used to**
388 **infer the vector velocity of the landslide. See online version for colour figure.**

389

390 **4.3. Characterising landslide run-out to enhance hazard assessments**

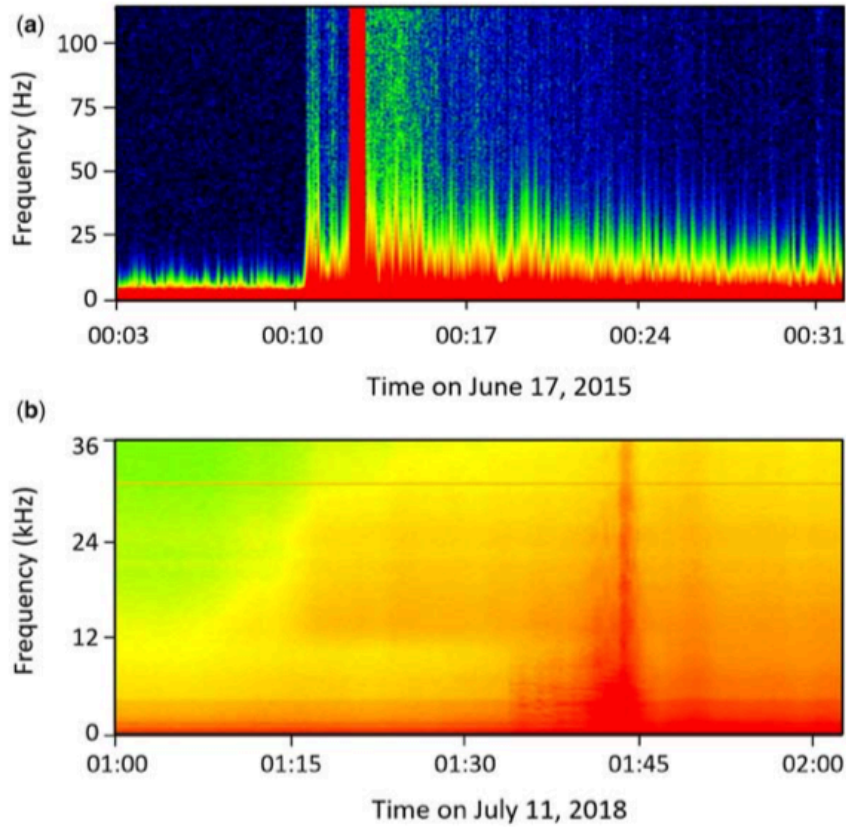
391 Submarine landslide run-out is often far more extensive than that on land, and may evolve dramatically
392 with regard to its rheology, as flows mix with seawater and/or entrain seafloor sediment (Parker, 1982;
393 Zeng et al., 1991; Mohrig and Marr, 2003; Gee et al., 2006; Heerema et al., 2020). As these mass flows
394 can travel at high speeds and across large distances, they can damage sensors placed in their path (e.g. see
395 several examples in Clare et al., 2020). Therefore the use of passive, remote sensing acoustic and seismic
396 monitoring tools, placed out of the direct pathway of such flows, can enable undisturbed monitoring and
397 reduce instrument damage or loss. Recent studies have demonstrated how hydrophones may record
398 turbidity currents (some of which were triggered by landslides) in fjord settings that are fed by seasonally
399 active rivers, including on the Fraser and Squamish deltas; both in British Columbia (Lintern et al., 2016;
400 2019; Hizzett et al., 2018; Hay et al., 2021; Figure 6). At the Fraser Delta, hydrophones are deployed on a
401 seafloor observatory that is connected to shore via the VENUS cabled network, enabling real-time
402 streaming of data, which also includes measurements by complementary active source geophysical
403 sensors (Lintern and Hill, 2010). Sensors such as Acoustic Doppler Current Profilers, provide the
404 calibration and confidence that the acoustic signals (which include both high (1-300 kHz) and low (Hz)
405 frequency ranges) can be attributed to turbidity currents (Lintern et al., 2016; 2019). At the Squamish
406 Delta, a hydrophone suspended from a vessel, 10 m above an active submarine channel, recorded the
407 noise generated from sixteen turbidity currents that reached speeds of 2 m/s (Hay et al., 2021). Extensive
408 calibration was provided by a pair of 500 kHz multibeam sonars placed on the same frame as the

409 hydrophone, three echosounders (28, 200 and 70-110 kHz) mounted on the vessel itself, and a 1200 kHz
410 ADCP suspended from a separate frame, also 10 m above the seafloor (15 m from the hydrophone
411 frame). This novel study showed that where turbidity currents exceeded 1 m/s, they generated noise well
412 above ambient ocean conditions, across a spectrum of 10-500 kHz; interpreted to result from highly
413 energetic sand-sized particle collisions. Cross-reference of hydrophone and ADCP-derived velocity
414 measurements, revealed that spectral density (at 100 kHz frequencies) is proportional to the speed of the
415 flow front, where a 100-fold increase in spectral density relates to a doubling in frontal speed (Figure 7;
416 Hay et al., 2021). Even more powerful sediment flows (i.e. >2 m/s, and potentially >10 m/s) that occur
417 within larger submarine canyons and channels (e.g. Carter et al., 2014; Azpiroz et al., 2017; Paull et al.,
418 2018), or that travel vast distances across open continental slopes (e.g. Piper et al., 1999), may generate
419 similar acoustic signals, and/or are likely to also generate ground motions (depending on their velocity,
420 interaction with, and the nature of the surrounding topography and seafloor substrate) that can be detected
421 with seismometers, but this requires future investigation.

422

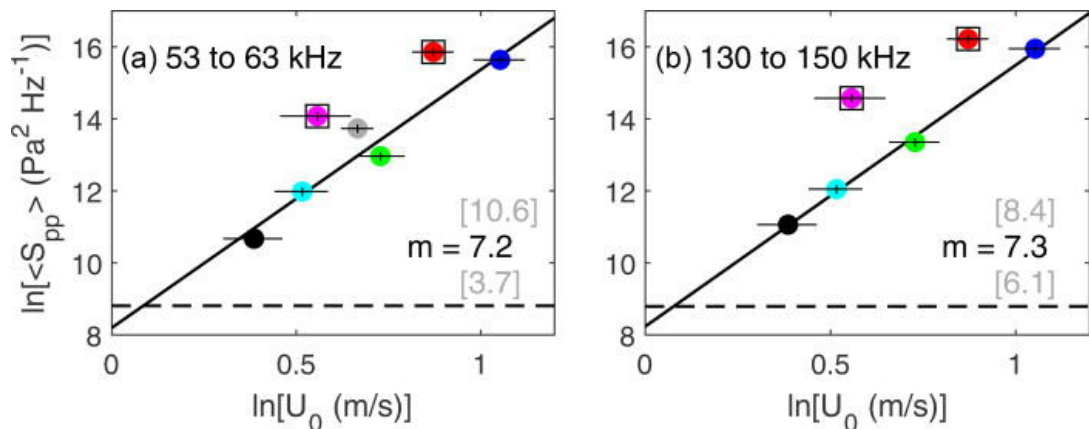
423 Seafloor cabled-networks, such as the Neutrino Mediterranean Observatory-Submarine Network 1
424 (NEMO-SN1), have demonstrated that offshore seismic monitoring can also play a future role in
425 detecting the run-out from submarine landslides. While background environmental noise was often found
426 to complicate conclusive signal identification, high frequency and long duration (at least longer than that
427 of earthquakes) signals recorded by an ocean bottom broadband seismometer on the NEMO-SN1 network
428 offshore Mount Etna were attributed to submarine landslide run-out (Sgroi et al., 2014). Therefore, this
429 approach can apparently be readily applied using marine seismometer networks, and similar deployment
430 of more than one seismometer would allow for greater characterization of events, including pin-pointing
431 their source. These recordings were of particularly high quality because the dedicated installation
432 procedure using a Remotely Operated Vehicle ensured excellent coupling with the seafloor. This is not
433 always the case for Ocean Bottom Seismometer surveys, as these instruments are typically dropped from
434 a surface vessel and land in a relatively uncontrolled manner on the seafloor.

435



436

437 **Figure 6: Hydrophone spectrograms showing turbidity current events in British Columbia. (a)**
 438 **Passing directly through a hydrophone at the delta dynamics laboratory at the Fraser Delta. (b)**
 439 **Passing below a mooring in the Bute Inlet Channel, British Columbia from Lintern et al. (2019).**
 440 **See online version for colour figure.**



441

442

443 **Figure 7: Cross-comparison of band-averaged noise spectral densities (S_{pp}) with frontal velocities**

444 **(U_0) of turbidity currents recorded in the Squamish Delta, British Columbia for two frequency**

445 **bands (from Hay et al., 2021). Coloured symbols represent different turbidity current events. Solid**
446 **black line is a best-fit trend and the dashed black line shows the detection threshold above ambient**
447 **noise levels. See online version for colour figure.**

448

449 **4.4. Opportunities using distributed cable-based sensing**

450 Spatially-resolved distributed sensing along seafloor fibre-optic cables now enables broadband seismic
451 and acoustic monitoring across long distances (over 10s-100s of km). Several recent studies have
452 demonstrated temporally- and spatially-resolved monitoring of ground motion (acting like distributed
453 networks of seismometers) generated by earthquakes, fault displacements, and acoustic noise created by
454 ocean waves and deep-sea bottom currents that resuspend sediment at the seafloor (e.g. Blum et al., 2010;
455 Marra et al., 2018; Ajo-Franklin et al., 2019; Lindsey et al., 2019; Williams et al., 2019; Zhan et al., 2020;
456 Nishimura et al., 2021; Zhan et al., 2021; Wilcock, 2021; Figure 8). Distributed acoustic sensing data
457 acquired along a fibre-optic cable in the Nankai subduction zone, western Japan, was found to have a
458 comparable performance to adjacent broadband ocean bottom seismometers at seismic frequencies of >1
459 Hz, provided the cable was well-coupled to the seafloor (Ide et al., 2021). The same study concluded that,
460 even though such distributed acoustic monitoring records one component of strain, seismic source
461 localisation within tens of kilometres of the cable can still be achieved. At lower frequencies (i.e. 0.02-
462 0.05 Hz) the distributed acoustic sensing observations were notably noisier compared to those from ocean
463 bottom seismometers, thus making detection of such events challenging, unless events occur very close to
464 the cable. The low frequency regime may be critical regional scale landslide detection (i.e. Fan et al.,
465 2020); hence this technique may be most appropriate for detecting relatively local low or far-field high
466 frequency signals, but more studies are required that provide similar comparisons, to test the sensitivities
467 of different cable configurations, interrogator units and analytical approaches (Lindsey and Martin, 2021;
468 Lior et al., 2021).

469

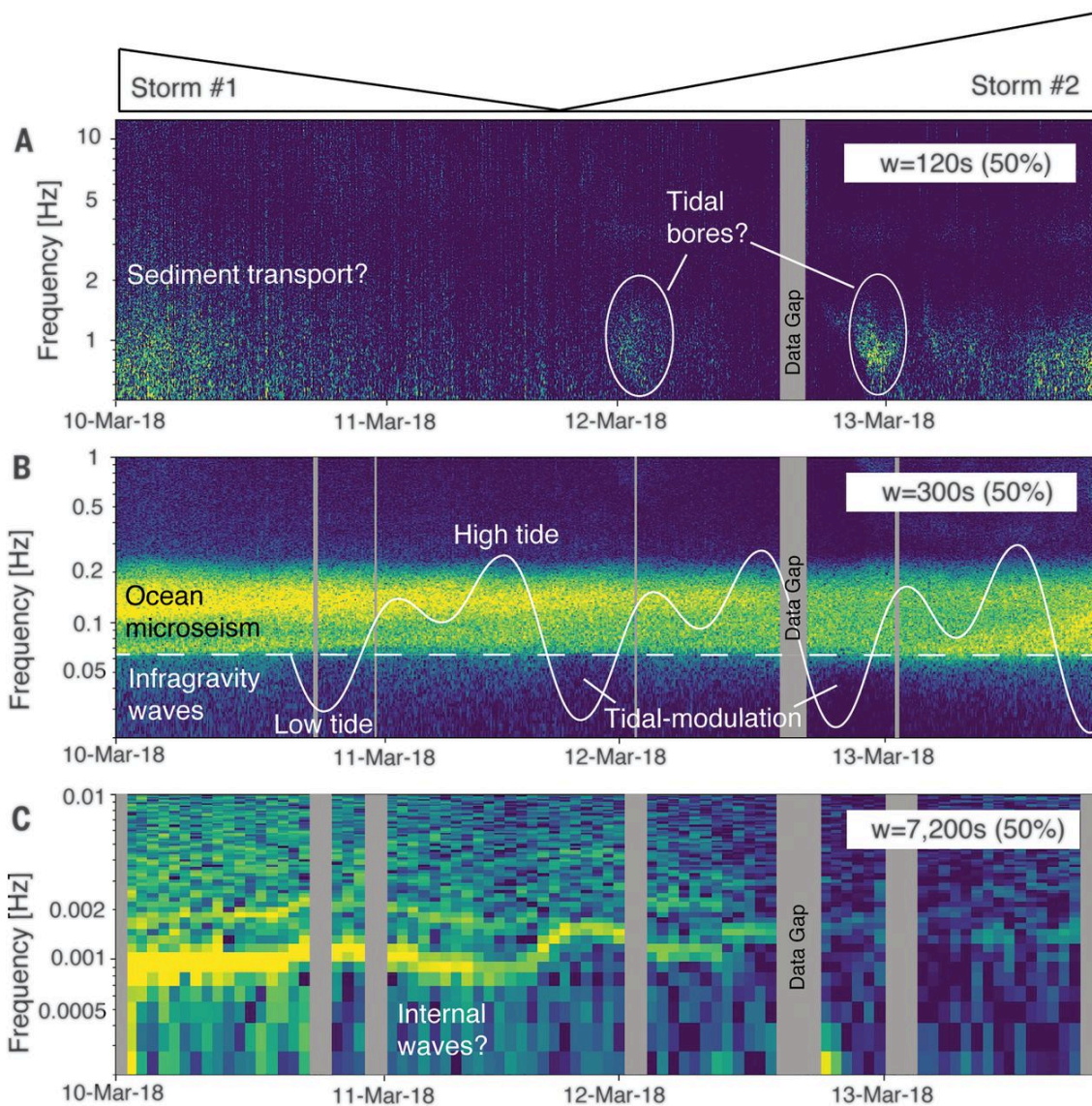
470 Recent advances have seen the application of sensing to detect changes in the State of Polarisation over
471 the full length of a 10,000 km-long telecommunications cable, which enabled recording of moderate to
472 large earthquakes, as well as pressure signals from ocean swells (thus illustrating the potential for real-

473 time tsunami detection over transoceanic distances; Zhan et al., 2021). This distance far exceeds that
474 reached by previous studies and did not require specialist interrogator units or ultra-stable laser sources;
475 instead monitoring the State of Polarisation to detect anomalies that are attributed to strong seismic waves
476 or long-period water waves (Zhan et al., 2021). It should be noted, however, that these long-range
477 measurements were spatially integrated (i.e. averaged along the entire fibre length); hence, additional,
478 independent information is required to locate and further characterise the hazard, besides the locally-
479 recorded signal timing and magnitude. Zhan et al. (2021) also recognised that site-specific effects can
480 affect the sensitivity of measurements, wherein the seabed coupling and nature of the seabed substrate on
481 which the cable is placed can result in spatially variable signal attenuation. Indeed, the coupling of the
482 cable with the seafloor may be particularly important for cable-based sensing. When assessing the
483 efficacy of Distributed Acoustic Sensing to detect earthquakes, Lioer et al. (2021) found that performance
484 was notably reduced in areas of highly irregular, rocky seafloor, where the cable is locally in free span,
485 raised above the seafloor across sections, and enhanced in areas of low relief, soft seafloor, particularly
486 where cables may become embedded or buried by sedimentation. Going forwards, cable sensing is likely
487 to be complimentary to other approaches, but also has strong potential to fill in major geographic gaps in
488 seismic monitoring, potentially making use of the existing global network of submarine cables and
489 accessing new cables (Ranasinghe et al., 2018; Howe et al., 2019; Mizutani et al., 2020; Mecozzi et al.,
490 2021; Wilcock, 2021).

491

492 While Distributed Acoustic Sensing can provide valuable information, such sensing is limited to no more
493 than a few hundred km from shore; hence, additional sensors, that could include hydrophones or
494 geophones, distributed at nodal locations along a cable may help to fill this gap over longer distances.
495 This is the premise of the SMART (Science Monitoring and Reliable Telecommunication) Cables
496 initiative, which proposes attaching instruments, including ground motion, pressure and temperature
497 sensors, as external nodes on repeaters (typically spaced 60-80 km apart) on new or decommissioned
498 submarine telecommunication cables (Ranasinghe et al., 2018; Howe et al., 2019; Mecozzi et al., 2021).
499 The CAM (Continent-Azores-Madeira) Ring cable is likely to be the first operational SMART Cable
500 system (coming online in 2024), connecting mainland Portugal with the Azores. As these nodes are

501 powered and connected by cables, they will potentially provide opportunities for real-time seismo-
502 acoustic monitoring far from shore. This is particularly relevant for the CAM Ring cable, as the strongest
503 earthquakes occur far offshore, and many of the previously mapped submarine landslides are located on
504 the flanks of remote submerged seamounts (Gamboa et al., 2021; Matias et al., 2021). Numerical
505 modelling indicates that the CAM Ring SMART cable should significantly reduce uncertainty in
506 pinpointing the location and timing of offshore earthquakes and identify events (such as submarine
507 landslides) that are currently undetectable by the existing onshore and coastal monitoring networks, while
508 detection of the passage and direction of tsunamis should provide improved early warning of coastal
509 impacts, and thus time to prepare emergency responses (Matias et al., 2021).



510

511 **Figure 8: Frequency spectrograms from Distributed Acoustic Sensing along a seafloor fibre optic**
512 **cable offshore Monterey Bay, California from Lindsey et al., 2019. These demonstrate how this**
513 **technique can be used to detect: A) short-lived tidal and near-bed currents; B) tidal effects due to**
514 **pressure changes; C) and internal waves. Therefore, this approach may also be appropriate to**
515 **measure aspects such as the run-out of submarine landslides (e.g. turbidity currents), displaced**
516 **water masses in front of a moving mass or ground motions generated by the landslide itself. See**
517 **online version for colour figure.**

518

519 **5. The application of passive geophysical monitoring in advancing submarine landslide science**

520 We now revisit the overarching challenges and science questions that were outlined in the introductory
521 section, specifically addressing how emerging seismic and acoustic techniques can fill outstanding
522 knowledge and capacity gaps, which uncertainties remain, and outline a proposed strategy for the forward
523 steps to advance submarine landslide science.

524

525 **5.1. Can passive seismic and acoustic techniques overcome the logistical challenges that have** 526 **previously-hindered monitoring of submarine landslides?**

527 First, we respond to the logistical challenges; namely the often-deep water and remote location of
528 submarine landslides, and their unpredictable and powerful nature. Provided sensors and receivers are
529 protected in appropriate pressure housing, passive seismo-acoustic landslide monitoring using
530 hydrophones and geophones can be performed across the full range of water depths in the global ocean,
531 from coastal (e.g. Hay et al., 2021) to thousands of metres water depth (e.g. Caplan-Auerbach et al.,
532 2014). To date, we are not aware of any landslide monitoring in hadal water depths, but it is certainly
533 logistically possible, and the use of ocean bottom seismometers and Distributed Acoustic Sensing along
534 fibre-optic cables is increasing in many deep ocean settings to record earthquake and non-earthquake
535 related noise (e.g. >4000 m offshore Chile, Batsi et al., 2019; Ide et al., 2021). Given the relatively early
536 stages of many the techniques we have described, most previous studies have relied upon individual
537 instruments, or limited networks of seabed or moored instruments, with narrow spatial coverage. Hence,
538 widespread (i.e. basin- to ocean-scale) passive monitoring of submarine landslides very much remains an

539 open and future challenge. However, onshore seismic monitoring networks are far more dense than those
540 offshore and, where margin geometry permits, these can immediately be used to identify submarine
541 landslides that may occur hundreds to thousands of kilometres from shore, where their location is not
542 known *a priori* (Fan et al., 2020).

543

544 The Gulf of Mexico is perhaps an ideal candidate, as its physiographic geometry suits the use of
545 triangulation from an onshore network to pinpoint the offshore location of submarine landslides. Arc-
546 shaped convergent continental margins are also good future candidates for this approach, as are enclosed
547 basins such as the Mediterranean, as they provide similarly well-suited geometries, and are often
548 themselves ‘blind spots’ for landslide-tsunami hazard where new insights are required (e.g. Sunda Arc;
549 Goff and Terry, 2016). The geometry of many margins will not suit this approach, however. As
550 recognised by Lin (2015), deployment of wider and denser networks of onshore and offshore
551 seismometers will be required in such settings for limitations to be overcome. Distributed Acoustic
552 Sensing along fibre-optic cables provides opportunities for long distance monitoring, and potentially to
553 fill several spatial gaps in offshore monitoring capacity, however, this technology cannot currently be
554 extended beyond the first repeater, and is thus presently limited over distances of less than a few hundreds
555 of kilometres from shore (Matias et al., 2021). This means that many submarine landslides, which occur
556 far offshore, cannot yet be recorded by this technique. Longer range (i.e. tens of thousands of kilometres)
557 monitoring is possible along cables that connect continents, either as integral measurements with limited
558 spatial resolution (e.g. Marra et al., 2018; Zhan et al., 2021), or at powered SMART sensor nodes along
559 the cable (e.g. Howe et al., 2019).

560

561 All of the passive monitoring approaches enable placement of sensing equipment out of the path of
562 submarine landslides and their run-out, which has hindered many previous efforts where sensors,
563 moorings and platforms have been damaged or lost (e.g. Khripounouff et al. 2003; Clare et al., 2020 and
564 references therein). These new techniques therefore ensure that not only the timing initiation of a
565 landslide can be recorded, but measurements can also be made during the landslide event itself, from
566 which key aspects of landslide behaviour can be determined.

567

568 **5.2. Which aspects of submarine landslides can we currently assess from passive remote sensing**
569 **techniques and what needs to be resolved?**

570 **5.2.1. Landslide timing**

571 The timing of submarine landslides has been determined from signals detected by submerged
572 hydrophones and geophones, as well as land-based seismic monitoring systems. Therefore, observational
573 passive monitoring datasets can provide new insights into the timing and frequency of submarine
574 landslides; starting to fill a key knowledge gap. For example, the use of land-based seismic monitoring in
575 the Gulf of Mexico identified 85 previously-undetected submarine landslide events (Fan et al., 2020). The
576 ability to identify past submarine landslide signals provides important information to develop more robust
577 hazard assessments and inform resilient routing and siting of offshore infrastructure (Chaytor et al.,
578 2020), while the quick identification of landslide signals has potential to enhance existing tsunami
579 warning systems (Fan et al., 2020; Matias et al., 2021). An immediate opportunity lies in back-analysis of
580 legacy datasets, to explore whether past landslide signals exist, but have been ignored by previous studies
581 as they focused on different frequency spectral ranges. Such an approach has already shown value in
582 identifying gas or fluid flow-related processes from ocean bottom seismometers or ocean currents from
583 Distributed Acoustic Sensing datasets (Baksi et al., 2019).

584

585 **5.2.2. Landslide triggers and preconditioning**

586 In addition to determining whether a landslide has occurred or not, ascertaining the timing of landslide
587 inception allows us to investigate the environmental conditions in the build up to that event; and thus
588 determine likely triggering and/or preconditioning factors. Limitations in the precise determination of
589 submarine landslide timing (e.g. due to uncertainties in radiocarbon dating) has hindered identification of
590 these links previously, but this is now possible, as highlighted by acoustic and seismic monitoring prior of
591 the 2018 Anak Krakatau volcanic collapse (Walter et al., 2019) and offshore landslides following
592 earthquakes in Taiwan (Lin, 2005). Future monitoring is likely to lead to the identification of new or
593 potentially surprising triggers, such as the intriguing link between distant earthquakes and submarine
594 landslides in the Gulf of Mexico (Fan et al., 2020). Passive monitoring technology is now sufficiently

595 mature to test previous hypotheses on landslide triggering and investigate new ones; however, operational
596 early warning systems (i.e. that automatically raise alerts ahead of a potential landslide event) still
597 remains a future prospect for all but a few locations, as this requires a robust understanding of the
598 conditions prior to failure or identification of a landslide as it happens. This will therefore be more
599 feasible at sites where triggers and/or preconditioning are more predictable and closely linked to
600 enhanced sediment supply from rivers (i.e. where landslides are more prone during or following periods
601 of higher river discharge, such as the bedload-dominated Fraser or Squamish Delta; Lintern et al., 2020;
602 Hay et al., 2021) or relate to heightened volcanic activity (e.g. Anak Krakatau, Indonesia; Mount Etna,
603 Mediterranean; Urlaub et al., 2018; Walter et al., 2019).

604

605 **5.2.3. Landslide location**

606 It is possible to pinpoint the location of submarine landslides through triangulation (to a precision of
607 approximately tens of kms; Caplan-Auerbach et al., 2014; Lin, 2015; Fan et al., 2020); however, as
608 already noted, this approach is limited to locations where sensor networks are sufficiently widely and
609 densely distributed. There is a wealth of existing onshore (and to a limited extent offshore) broadband
610 seismic datasets in several regions where the same approach could be taken, to investigate whether
611 similar landslide-like signals exist, if they can be located spatially, and if they correspond to any of the
612 recent direct measurements of slope instability and their run-out, or existing maps of landslide
613 vulnerability (e.g. Paul et al., 2018; Urlaub et al., 2018; Obelcz et al., 2020; Gamboa et al., 2021). We
614 suggest that detailed bathymetric surveys should be performed in areas where seismic signals attributed to
615 submarine landslides have been located to determine which types of landslide are recorded, as well as to
616 the test the efficacy of landslide detection. The Gulf of Mexico, Mediterranean, Caribbean and regions
617 offshore south-west Taiwan are prime candidates for this field calibration.

618

619 **5.2.4. Landslide kinematics**

620 If a landslide mass is known, it is possible to infer other aspects of submarine landslide behaviour from
621 the resultant seismic and acoustic signals. For instance, inversion of these signals can be used to derive
622 force histories, from which volume, velocity, changes in basal friction, run-out distance, and other

623 important aspects of landslide kinematics can be determined, as demonstrated by successful application of
624 these approaches in terrestrial settings (e.g. Brodsky et al., 2003; Ekström and Stark, 2013; Yamada et al.,
625 2013; Moretti et al., 2015). These aspects will likely be more challenging to constrain than landslide
626 timing and location, however; requiring concerted research and field calibration. Sites where passive and
627 active monitoring are performed concurrently will provide valuable opportunities to calibrate the nature
628 of seismic and/or acoustic signals, such as at the Squamish Delta, Canada, where variations in noise
629 spectra were linked to changes in the concentration and grain size of sediment avalanches, and noise
630 intensity corresponded to the velocity of the flow front of turbidity currents (Hay et al., 2021). Moored
631 arrays of direct active sensors (e.g. ADCPs) have been used to track the passage and evolution of
632 landslide run-out and turbidity currents down submarine canyons, over tens of kilometres (e.g. Paull et
633 al., 2018). The addition of co-located hydrophones and geophones to such moored or seafloor arrays will
634 enable calibration of seismic and acoustic signals as well as determining threshold limits for detection.

635

636 **5.2.5. Site-specific effects**

637 We suggest that different deployment configurations should be trialed to investigate how signals attenuate
638 in different settings, as well as investigating the effects of increasing distance and differing angles of
639 incidence from source. The effects of seafloor morphology may attenuate the signal generated by
640 submarine landslides and complicate its propagation pathway, which is particularly important for
641 directional instruments such as hydrophones. While hydrophones have been shown to detect events on
642 relatively open delta slopes (Hay et al., 2021), to what extent the topographic effects of deeply-incised
643 submarine canyons may limit detection of events by similar sensors placed outside the canyon, along
644 narrow fjords or other irregular seafloor terrain remains poorly constrained. It is also important to identify
645 and differentiate landslide-related noise from ambient seismic and acoustic noise that arises from natural
646 background processes and human activities in the ocean. In noisy marine environments, ambient noise
647 may overprint or entirely obscure the records of submarine landslides; hence, an understanding of the
648 levels, frequency and time windows of that background noise is important when designing monitoring
649 strategies (Lior et al., 2021). Societal lockdowns in 2020 and 2021 associated with the COVID-19
650 pandemic have been identified as periods of significantly reduced seismic noise both on land and at sea

651 (Lecocq et al., 2020; Ryan et al., 2020), and may therefore provide a rare window of reduced background
652 noise to explore local to global datasets. If signals can be sufficiently calibrated and confidently attributed
653 to submarine landslides, historical records can be re-analysed to extend landslide catalogues in many
654 regions worldwide, adding significant value to already valuable legacy datasets and providing new
655 avenues for research and informing hazard management strategies.

656

657 **5.2.6. Challenges in data transfer**

658 As passive geophysical systems require much less power than active sensors (e.g. such as ADCPs), they
659 can improve the endurance of offshore monitoring, lengthening monitoring windows in time. Future
660 challenges still lie in transmission of data from sites that are far from shore (i.e. in abyssal to hadal water
661 depths), particularly if an end goal is to support early-warning systems. This issue is largely moot for
662 cabled systems as they support high bandwidth data transfer; although as already noted, the current reach
663 of Distributed Acoustic Sensing limits long distance (>100s of km) monitoring. For ocean bottom
664 seismometers or hydrophones on seabed frames or moorings, there is currently no simple solution, as data
665 file sizes typically exceed that currently permissible by acoustic data transmission.

666

667 **5.3. Suggestions for future directions**

668 We now finish by making some specific suggestions with regards to the future activities, listed in a
669 broadly prioritised order.

670

671 **5.3.1. Focus on calibration of hydrophone and geophone records at specific, well-known, 672 active sites**

673 We suggest that efforts should be focused on specific sites and settings to provide the calibration needed
674 to strengthen confidence in the characterisation of submarine landslides from passive monitoring data. It
675 is sensible to target active sites where previous monitoring has demonstrated regular landslide activity,
676 where pre- and post-event bathymetric data are available, and where passive instruments (hydrophones,
677 geophones, fibre-optic cables etc.) can be deployed concurrently with active sensors that record key
678 parameters such as event timing, subsurface pore pressure, elevation changes, and flow velocity and

679 sediment concentration. The Fraser Delta is one such location, being connected by seafloor cables to
680 Ocean Networks Canada's VENUS network (that enable real-time data transfer to shore) in an area of
681 high sediment supply with sub-annual landslide activity. Synchronous deployment of hydrophones and
682 seismometers, with current meters, inclinometers and piezometers (among other sensors) provides an
683 ideal test bed for calibrated interpretation of seismic and acoustic signals attributed to small-scale
684 submarine landslides (Lintern and Hill, 2010; Lintern et al, 2020). Other cable-connected sites, such as
685 the EMSO (European Multidisciplinary Seafloor and water column Observatory) Ligure-Nice
686 observatory provide opportunities to monitor the development of potential precursor conditions, but
687 landslide recurrence is orders of magnitude lower at this site compared to the Fraser Delta; hence, the
688 likelihood of catching a landslide itself is much less likely (Bompais et al., 2019). Similarly, the DONET
689 (Dense Oceanfloor Network system for Earthquakes and Tsunamis) cabled sensor network located
690 offshore SW Japan provides opportunities to detect submarine landslides, but intriguingly no evidence for
691 such activity was found within a few hours of two large ($>6 M_w$) earthquakes, with a study concluding
692 that slopes may not be particularly susceptible to slope failure in that region (Gomberg et al., 2021).
693 Indeed, most cabled observatories tend to avoid areas of very frequent landslide activity, so it will also be
694 necessary to perform field calibration in other settings using more conventional landers or moorings that
695 are not connected by cables, which requires sea-going research cruises. Sites with high, and predictable,
696 sediment supply and where active field campaigns are planned will be the preferred candidates for
697 synchronous deployment of active and passive monitoring equipment, such as major submarine canyons
698 that connect to large rivers, or whose head intersects seasonally-variable littoral transport cells (e.g.
699 canyons where sub-annual turbidity currents have previously been recorded: Congo Canyon, West Africa;
700 Gaoping Canyon, Taiwan; Var Canyon, Mediterranean; Capbreton Canyon, Bay of Biscay; Khripounoff
701 et al. 2012; Azpiroz-Zabala et al., 2017; Paull et al., 2018; Zhang et al., 2018). On a larger-scale, it will
702 also be important to acquire data at active volcanic sites where onshore and offshore monitoring is on-
703 going, such as the geodetic monitoring offshore Mount Etna, or land-based acoustic emission and GPS
704 monitoring at Anak Krakatau (Urlaub et al., 2018; Walter et al., 2018). These activities should go hand in
705 hand with efforts to determine site-specific effects on attenuation (e.g. due to topographic, substrate and

706 other effects), which will benefit from numerical modelling to help identify and design the optimal sensor
707 (e.g. where is the strongest or earliest signal expected?).

708

709 **5.3.2. Explore and calibrate existing land-based seismic monitoring data**

710 We suggest that more can, and should be, made of legacy broadband seismic datasets to explore past
711 catalogues for evidence of submarine landslides. This method has been demonstrated offshore USA and
712 Taiwan (Lin, 2015; Fan et al., 2020) and is more widely applicable, using data that have already been
713 collected. Analysis of past time-series data should then be complemented with the acquisition of new
714 seafloor survey data, to confirm that the spatial locations of landslide signals do indeed correspond with
715 landslide events, and determine if a specific type(s) of landslide is more likely to generate a detectable
716 seismic signal. This calibration will be most effective in areas where detailed swath multibeam echo-
717 sounder surveys have already been performed (in particular high-resolution datasets acquired using
718 Autonomous Underwater Vehicles), as differential elevations between multiple surveys provide a time
719 window for a landslide, as well as its location. While repeat seafloor surveys are relatively rare, their use
720 is growing, particularly in active submarine canyons (e.g. Smith et al., 2007; Paull et al., 2018), volcanic
721 island flanks (e.g. Le Friant et al., 2010; Caplan-Auerbach et al., 2014; Hunt et al., 2021), offshore river
722 deltas (e.g. Lintern et al., 2016; Obelcz et al., 2017), including across the Mississippi submarine delta
723 where seafloor infrastructure is threatened by submarine slope failures (Chaytor et al., 2020; Obelcz et al.,
724 2020). The footprint of these surveys tends to be quite limited; hence, it will most likely be necessary to
725 target specific areas, focusing on acquiring high-resolution bathymetric data that enables identification of
726 landslide scars and/or deposits. Evidence of landslide impacts on seafloor infrastructure (e.g. cable
727 breaks, pipeline damage) may provide a useful addition point of calibration as this provides constraint on
728 both timing and location of the event (e.g. Carter et al., 2014). Analysis of legacy seismic monitoring
729 datasets, as well as new ones, will benefit from application of emergent machine learning techniques that
730 permit analysis of vast datasets to train algorithms to automatically identify landslide events, and
731 potentially identify previously-unrecognised environmental patterns that relate to landslide
732 preconditioning (Thirugnanam et al., 2020; Deng et al., 2021).

733

734 **5.3.3. Calibrate and test fibre-optic detection of submarine landslides**

735 The emergence of fibre-optic sensing to monitor offshore geohazards (in particular Distributed Acoustic
736 Sensing) is an exciting prospect, but one that currently remains unproven at field-scale for submarine
737 landslide detection. The frequency ranges for detection appear to largely fall within the capabilities of
738 Distributed Acoustic Sensing, although confident identification of low frequency ($\ll 1$ Hz) signals may
739 be challenging, particularly in noisy environments (e.g. due to natural ocean processes and human
740 activities) or where cables are poorly coupled with the seafloor. Synchronous deployment of arrays of
741 ocean bottom seismometers and hydrophones in active landslide settings are needed to provide the
742 confidence in interpretation of Distributed Acoustic Sensing data as well as assessing the distance (both
743 along-cable, and adjacent to it) over which measurements can reliably be made of the different signals
744 created by submarine landslides. When installing new pipelines and cable, or when seafloor structures are
745 decommissioned and left in situ, consideration could be given to integrate passive monitoring
746 instrumentation to complement that used for monitoring infrastructure integrity (Wilcock et al., 2021). As
747 SMART cables are installed (planned from 2024), opportunities will arise for accessing distributed sensor
748 packages that may include hydrophones and/or geophones, adding valuable new potential locations for
749 submarine landslide detection (Howe et al., 2019; Matias et al., 2021).

750

751 **5.3.4. Extending the global monitoring network to enable operational early warning systems**

752 In the longer-term there is a need for expanded acoustic and seismic monitoring networks offshore; not
753 only for detection of submarine landslides, but also for a host of ocean and earth science applications
754 (Wilcock et al. 2021). Future opportunities may exist through collaboration with global monitoring
755 programmes, such as MERMAIDS (Mobile Earthquake Recording in Marine Areas by Independent
756 Divers), which employs a network of autonomous floats equipped with hydrophones (0.1-50 kHz) that
757 passively drift across the ocean for deployments lasting up to five years; capable of transmitting
758 seismograms in near real-time (Sukhovich et al., 2015; Hello and Nolet, 2020). Data gathered in such a
759 manner may provide useful opportunistic snapshots of certain aspects of landslide activity, but may only
760 yield limited data to answer outstanding science questions given the mobile nature of the floats and the
761 lack of ground motion data. Therefore static seafloor sensors, rather than floating ones, will also be

762 required, but a similar approach (i.e. that focuses developing low cost, and long endurance monitoring
763 platforms) is an important future direction. Whether seismic monitoring networks are extended offshore
764 attached to cables, via distributed fibre-optic sensing, or using stand-alone moorings, seafloor landers or
765 nodes, the development of more cost-effective sensors that do not require regular servicing, and are
766 capable of transmitting data remotely, will transform our ability to monitor and ultimately provide early
767 warning for submarine landslides. It is unlikely that we will fully rely upon passive monitoring
768 approaches, but a future outlook could include automated decision-making by smart networks that
769 determine whether a significant event has occurred, prompting the release of pop-up floats to transmit
770 data, or active (high power-use) systems that are triggered to start recording, or switch to a higher
771 sampling rate, by passive (lower power-use) sensors.

772

773 **6. Concluding remarks**

774 While there are still many open questions concerning submarine landslides and the hazards they pose, the
775 recent growth in marine geophysical monitoring is rapidly providing data to start filling many of those
776 gaps. Passive seismic and acoustic monitoring is in its relative infancy in this field, but has already shown
777 significant promise in enabling the detection of submarine landslides over large areas, to ascertain their
778 precise timing (and hence determine likely triggers), provide constraints on their transit velocity and run-
779 out distance, and their effects (e.g. tsunami generation). We consider that these longer endurance and
780 often more cost effective techniques are likely to form a complementary addition to existing approaches,
781 rather than replace them entirely, particularly as many aspects of landslides can generate ground motions
782 and/or acoustic noise. Ongoing calibration needs to be a priority to reliably discern and interpret signals
783 generated by submarine landslides. Greater understanding through modeling will help to identify optimal
784 sensor configurations. Distributed sensing along fibre-optic cables is an intriguing proposition, however,
785 there is a compelling need to understand precisely what a submarine landslide signal looks like and over
786 what spatial scale such signals can be reliably recorded. Studies are immediately required that test the
787 sensitivity of passive landslide detection (using onshore and offshore networks) through concurrent
788 deployment of active sensors. Once that calibration is performed across a breadth of sites and settings, we

789 suggest that passive seismic and acoustic monitoring has the potential to answer a host of key,
790 outstanding questions and significantly advance the field of submarine landslide science.

791

792 **7. Acknowledgements**

793 Clare and Talling acknowledge funding from the Natural Environment Research Council (NERC),
794 including ‘Environmental Risks to Infrastructure: Identifying and Filling the Gaps’ (NE/ P005780/1),
795 ‘New field-scale calibration of turbidity current impact modelling’ (NE/P009190/1), “Developing a
796 Global Listening Network for Turbidity Currents and Seafloor Processes” (NE/S009965/1 and
797 NE/S010068/1). The authors also acknowledge discussions with collaborators as part of Talling’s NERC
798 International Opportunities Fund grant (NE/M017540/1) ‘Coordinating and pump-priming international
799 efforts for direct monitoring of active turbidity currents at global test sites’. Clare also acknowledges
800 support from the International Cable Protection Committee. Talling was supported by a NERC and Royal
801 Society Industry Fellowship hosted by the International Cable Protection Committee. Additional funding
802 for Clare was provided by NERC National Capability Climate Linked Atlantic Sector Science
803 Programme (NE/R015953/1). E. Pope was supported by a Leverhulme Early Career Fellowship (ECF-
804 2018-267). We thank Bruce Howe and an anonymous reviewer for constructive feedback that improved
805 the manuscript.

806

807 **8. References**

- 808 Ai, F., Strasser, M., Preu, B., Hanebuth, T.J., Krastel, S. and Kopf, A., 2014. New constraints on
809 oceanographic vs. seismic control on submarine landslide initiation: a geotechnical approach off
810 Uruguay and northern Argentina. *Geo-Marine Letters*, 34(5), pp.399-417.
- 811 Ajo-Franklin, J.B., Dou, S., Lindsey, N.J., Monga, I., Tracy, C., Robertson, M., Tribaldos, V.R., Ulrich,
812 C., Freifeld, B., Daley, T. and Li, X., 2019. Distributed acoustic sensing using dark fiber for near-
813 surface characterization and broadband seismic event detection. *Scientific reports*, 9(1), pp.1-14.
- 814 Antsyferov, M.S., 1959. *Seismo-Acoustic Methods in Mining* (Consultants Bureau, New York, 1966);
815 SD Vinogradov. *Bull. Acad. Sci. USSR Geophys. Ser.*, 2.

816 Azpiroz-Zabala, M., Cartigny, M.J., Talling, P.J., Parsons, D.R., Sumner, E.J., Clare, M.A., Simmons,
817 S.M., Cooper, C. and Pope, E.L., 2017. Newly recognized turbidity current structure can explain
818 prolonged flushing of submarine canyons. *Science advances*, 3(10), p.e1700200.

819 Batsi, E., Tsang-Hin-Sun, E., Klingelhoefer, F., Bayrakci, G., Chang, E.T., Lin, J.Y., Dellong, D.,
820 Monteil, C. and Géli, L., 2019. Nonseismic Signals in the Ocean: Indicators of Deep Sea and Seafloor
821 Processes on Ocean-Bottom Seismometer Data. *Geochemistry, Geophysics, Geosystems*, 20(8),
822 pp.3882-3900.

823 Baumgartner, M.F., Stafford, K.M. and Latha, G., 2018. Near real-time underwater passive acoustic
824 monitoring of natural and anthropogenic sounds. In *Observing the Oceans in Real Time* (pp. 203-226).
825 Springer, Cham.

826 Besson, B., Eiríksson, G., Thórarinnsson, Ó., Thórarinnsson, A. and Einarsson, S., 2007. Automatic
827 detection of avalanches and debris flows by seismic methods. *Journal of Glaciology*, 53(182), pp.461-
828 472.

829 Biscara, L., Hanquiez, V., Leynaud, D., Marieu, V., Mulder, T., Gallissaires, J. M., Crespin, J.-P.,
830 Braccini, E. and Garlan, T. (2012). Submarine slide initiation and evolution offshore Pointe Odden,
831 Gabon-Analysis from annual bathymetric data (2004–2009). *Marine Geology*, 299, 43-50.

832 Blum, J.A., Chadwell, C.D., Driscoll, N. and Zumberge, M.A., 2010. Assessing slope stability in the
833 Santa Barbara Basin, California, using seafloor geodesy and CHIRP seismic data. *Geophysical*
834 *Research Letters*, 37(13).

835 Bompais, X., Garziglia, S., Blandin, J. and Hello, Y., 2019, June. EMSO-Ligure Nice, a Coastal Cabled
836 Observatory Dedicated to the Study of Slope Stability. In *OCEANS 2019-Marseille* (pp. 1-8). IEEE.

837 Brackenridge, R.E., Nicholson, U., Sapiie, B., Stow, D. and Tappin, D.R., 2020. Indonesian Throughflow
838 as a preconditioning mechanism for submarine landslides in the Makassar Strait. *Geological Society,*
839 *London, Special Publications*, 500(1), pp.195-217.

840 Brodsky, E.E., Gordeev, E. and Kanamori, H., 2003. Landslide basal friction as measured by seismic
841 waves. *Geophysical Research Letters*, 30(24).

842 Brothers, D.S., Luttrell, K.M. and Chaytor, J.D., 2013. Sea-level-induced seismicity and submarine landslide
843 occurrence. *Geology*, 41(9), pp.979-982.

844 Brooks, H.L., Hodgson, D.M., Brunt, R.L., Peakall, J. and Flint, S.S., 2018. Exhumed lateral margins and
845 increasing flow confinement of a submarine landslide complex. *Sedimentology*, 65(4), pp.1067-1096.

846 Bull, S., Arnot, M., Browne, G., Crundwell, M., Nicol, A. and Strachan, L., 2019. Neogene and
847 Quaternary Mass-Transport Deposits From the Northern Taranaki Basin (North Island, New Zealand)
848 Morphologies, Transportation Processes, and Depositional Controls. *Submarine Landslides:
849 Subaqueous Mass Transport Deposits from Outcrops to Seismic Profiles*, pp.171-180.

850 Bull, S., Cartwright, J. and Huuse, M., 2009. A review of kinematic indicators from mass-transport
851 complexes using 3D seismic data. *Marine and Petroleum Geology*, 26(7), pp.1132-1151.

852 Buss, C., Friedli, B. and Puzrin, A.M., 2019. Kinematic energy balance approach to submarine landslide
853 evolution. *Canadian Geotechnical Journal*, 56(9), pp.1351-1365.

854 Cadman, J.D. and Goodman, R.E., 1967. Landslide noise. *Science*, 158(3805), pp.1182-1184.

855 Campbell, C.S., Cleary, P.W. and Hopkins, M., 1995. Large-scale landslide simulations: Global
856 deformation, velocities and basal friction. *Journal of Geophysical Research: Solid Earth*, 100(B5),
857 pp.8267-8283.

858 Campbell, K.J., Kinnear, S. and Thame, A., 2015. AUV technology for seabed characterization and
859 geohazards assessment. *The leading edge*, 34(2), pp.170-178.

860 Caplan-Auerbach, J., Fox, C.G. and Duennebie, F.K., 2001. Hydroacoustic detection of submarine
861 landslides on Kilauea volcano. *Geophysical Research Letters*, 28(9), pp.1811-1813

862 Caplan-Auerbach, J. and Huggel, C., 2007. Precursory seismicity associated with frequent, large ice
863 avalanches on Iliamna volcano, Alaska, USA. *Journal of Glaciology*, 53(180), pp.128-140.

864 Caplan-Auerbach, J., Dziak, R.P., Bohnenstiehl, D.R., Chadwick, W.W. and Lau, T.K., 2014.
865 Hydroacoustic investigation of submarine landslides at West Mata volcano, Lau Basin. *Geophysical
866 Research Letters*, 41(16), pp.5927-5934.

867 Carter, L., Gavey, R., Talling, P.J. and Liu, J.T., 2014. Insights into submarine geohazards from breaks in
868 subsea telecommunication cables. *Oceanography*, 27(2), pp.58-67.

869 Casas, D., Chiocci, F., Casalbore, D., Ercilla, G. and De Urbina, J.O., 2016. Magnitude-frequency
870 distribution of submarine landslides in the Gioia Basin (southern Tyrrhenian Sea). *Geo-Marine
871 Letters*, 36(6), pp.405-414.

872 Chadwick Jr, W.W., Dziak, R.P., Haxel, J.H., Embley, R.W. and Matsumoto, H., 2012. Submarine
873 landslide triggered by volcanic eruption recorded by in situ hydrophone. *Geology*, 40(1), pp.51-54.

874 Chaytor, J.D., Baldwin, W.E., Bentley, S.J., Damour, M., Jones, D., Maloney, J., Miner, M.D., Obelcz, J.
875 and Xu, K., 2020. Short-and long-term movement of mudflows of the Mississippi River Delta Front
876 and their known and potential impacts on oil and gas infrastructure. *Geological Society, London,*
877 *Special Publications*, 500(1), pp.587-604.

878 Chichibu, A., Jo, K., Nakamura, M., Goto, T. and Kamata, M., 1989. Acoustic emission characteristics of
879 unstable slopes. *Journal of Acoustic Emission*, 8(4), pp.107-112.

880 Clare, M.A., Vardy, M.E., Cartigny, M.J., Talling, P.J., Himsworth, M.D., Dix, J.K., Harris, J.M.,
881 Whitehouse, R.J. and Belal, M., 2017. Direct monitoring of active geohazards: Emerging geophysical
882 tools for deep-water assessments. *Near Surface Geophysics*, 15(4), pp.427-444.

883 Clare, M., Lintern, D.G., Rosenberger, K., Clarke, J.E.H., Paull, C., Gwiazda, R., Cartigny, M.J., Talling,
884 P.J., Perara, D., Xu, J. and Parsons, D., 2020. Lessons learned from the monitoring of turbidity
885 currents and guidance for future platform designs. *Geological Society, London, Special*
886 *Publications*, 500(1), pp.605-634.

887 Clare, M., Chaytor, J., Dabson, O., Gamboa, D., Georgiopoulou, A., Eady, H., Hunt, J., Jackson, C., Katz,
888 O., Krastel, S. and León, R., 2019. A consistent global approach for the morphometric characterization
889 of subaqueous landslides. *Geological Society, London, Special Publications*, 477(1), pp.455-477.

890 Collico, S., Arroyo, M., Urgeles, R., Gràcia, E., Devincenzi, M. and Pérez, N., 2020. Probabilistic
891 mapping of earthquake-induced submarine landslide susceptibility in the South-West Iberian
892 margin. *Marine Geology*, 429, p.106296.

893 Cook, K.L., Andermann, C., Gimbert, F., Adhikari, B.R. and Hovius, N., 2018. Glacial lake outburst
894 floods as drivers of fluvial erosion in the Himalaya. *Science*, 362(6410), pp.53-57

895 Cook, K.L., Rekapali, R., Dietze, M., et al. 2021. Detection and potential early warning of catastrophic
896 flow events with regional seismic networks, *Science*, 374, 87-92.

897 Deng, L., Smith, A., Dixon, N. and Yuan, H., 2021. Machine learning prediction of landslide deformation
898 behaviour using acoustic emission and rainfall measurements. *Engineering Geology*, p.106315.

899 Deparis, J., Jongmans, D., Cotton, F., Baillet, L., Thouvenot, F. and Hantz, D., 2008. Analysis of rock-
900 fall and rock-fall avalanche seismograms in the French Alps. *Bulletin of the Seismological Society of*
901 *America*, 98(4), pp.1781-1796.

902 Dewey, J. W., & Dellinger, J. A. (2008). Location of the Green Canyon (offshore southern Louisiana)
903 seismic event of February 10, 2006, U.S. *Geological Survey Open-File Report*, 31p, 2008– 1194.

904 Dixon, N. and Spriggs, M., 2007. Quantification of slope displacement rates using acoustic emission
905 monitoring. *Canadian Geotechnical Journal*, 44(8), pp.966-976.

906 Dixon, N., Spriggs, M.P., Smith, A., Meldrum, P. and Haslam, E., 2015. Quantification of reactivated
907 landslide behaviour using acoustic emission monitoring. *Landslides*, 12(3), pp.549-560.

908 Downs, P.W., Soar, P.J. and Taylor, A., 2016. The anatomy of effective discharge: the dynamics of
909 coarse sediment transport revealed using continuous bedload monitoring in a gravel-bed river during a
910 very wet year. *Earth Surface Processes and Landforms*, 41(2), pp.147-161.

911 Dugan, B. (2012). Petrophysical and consolidation behavior of mass transport deposits from the northern
912 Gulf of Mexico, IODP Expedition 308. *Marine Geology*, 315, 98-107.

913 Ekström, G. and Stark, C.P., 2013. Simple scaling of catastrophic landslide
914 dynamics. *Science*, 339(6126), pp.1416-1419.

915 Fan, W., McGuire, J.J. and Shearer, P.M., 2020. Abundant spontaneous and dynamically triggered
916 submarine landslides in the Gulf of Mexico. *Geophysical Research Letters*, 47(12),
917 p.e2020GL087213.

918 Frey-Martínez, J., Cartwright, J. and James, D., 2006. Frontally confined versus frontally emergent
919 submarine landslides: A 3D seismic characterisation. *Marine and Petroleum Geology*, 23(5), pp.585-
920 604.

921 Fujiwara, T., dos Santos Ferreira, C., Bachmann, A.K., Strasser, M., Wefer, G., Sun, T., Kanamatsu, T.
922 and Kodaira, S., 2017. Seafloor displacement after the 2011 Tohoku-Oki earthquake in the northern
923 Japan trench examined by repeated bathymetric surveys. *Geophysical Research Letters*, 44(23), pp.11-
924 833.

925 Galitzin, B., 1915. Sur l'angle d'emergence des rayons sismiques. *Bull.(Izv.) Central Seismic Commission*
926 *Russian Academy of Science*, 7(2).

927 Gamboa, D., Omira, R. and Terrinha, P., 2021. A database of submarine landslides offshore West and
928 Southwest Iberia. *Scientific Data*, 8(1), pp.1-9.

929 Geay, T., Belleudy, P., Gervaise, C., Habersack, H., Aigner, J., Kreisler, A., Seitz, H. and Laronne, J.B.,
930 2017. Passive acoustic monitoring of bed load discharge in a large gravel bed river. *Journal of*
931 *Geophysical Research: Earth Surface*, 122(2), pp.528-545.

932 Geay, T., Zanker, S., Misset, C. and Recking, A., 2020. Passive Acoustic Measurement of Bedload
933 Transport: Toward a Global Calibration Curve?. *Journal of Geophysical Research: Earth*
934 *Surface*, 125(8), p.e2019JF005242.

935 Gee, M.J.R., Gawthorpe, R.L. and Friedmann, J.S., 2005. Giant striations at the base of a submarine
936 landslide. *Marine Geology*, 214(1-3), pp.287-294.

937 Gee, M.J.R., Gawthorpe, R.L. and Friedmann, S.J., 2006. Triggering and evolution of a giant submarine
938 landslide, offshore Angola, revealed by 3D seismic stratigraphy and geomorphology. *Journal of*
939 *Sedimentary Research*, 76(1), pp.9-19.

940 Geist, E.L. and Parsons, T., 2010. Estimating the empirical probability of submarine landslide occurrence.
941 In *Submarine mass movements and their consequences* (pp. 377-386). Springer, Dordrecht.

942 Goff, J. and Terry, J.P., 2016. Tsunamigenic slope failures: the Pacific Islands ‘blind
943 spot’?. *Landslides*, 13(6), pp.1535-1543.

944 Gomberg, J., Ariyoshi, K., Hautala, S. and Johnson, H.P., The Finicky Nature of Earthquake Shaking-
945 Triggered Submarine Sediment Slope Failures and Sediment Gravity Flows. *Journal of Geophysical*
946 *Research: Solid Earth*, p.e2021JB022588.

947 Guiastrennec-Faugas, L., Gillet, H., Peakall, J., Dennielou, B., Gaillot, A. and Jacinto, R.S., 2021.
948 Initiation and evolution of knickpoints and their role in cut-and-fill processes in active submarine
949 channels. *Geology*, 49(3), pp.314-319.

950 Hampton, M.A., Lee, H.J. and Locat, J., 1996. Submarine landslides. *Reviews of geophysics*, 34(1),
951 pp.33-59.

952 Harbitz, C.B., Løvholt, F. and Bungum, H., 2014. Submarine landslide tsunamis: how extreme and how
953 likely?. *Natural Hazards*, 72(3), pp.1341-1374.

954 Hay, A.E., Hatcher, M.G. and Hughes Clarke, J.E., 2021. Underwater noise from submarine turbidity
955 currents. *JASA Express Letters*, 1(7), p.0

956 Heerema, C.J., Talling, P.J., Cartigny, M.J., Paull, C.K., Bailey, L., Simmons, S.M., Parsons, D.R., Clare,
957 M.A., Gwiazda, R., Lundsten, E. and Anderson, K., 2020. What determines the downstream evolution
958 of turbidity currents?. *Earth and Planetary Science Letters*, 532, p.116023.

959 Heijnen, M.S., Clare, M.A., Cartigny, M.J., Talling, P.J., Hage, S., Lintern, D.G., Stacey, C., Parsons,
960 D.R., Simmons, S.M., Chen, Y. and Sumner, E.J., 2020. Rapidly-migrating and internally-generated
961 knickpoints can control submarine channel evolution. *Nature communications*, 11(1), pp.1-15.

962 Hello, Y. and Nolet, G., 2020. Floating seismographs (MERMAIDS). *Encyclopedia of Solid Earth*
963 *Geophysics*, pp.1-6.

964 Hibert, C., Michéa, D., Provost, F., Malet, J.P. and Geertsema, M., 2019. Exploration of continuous
965 seismic recordings with a machine learning approach to document 20 yr of landslide activity in
966 Alaska. *Geophysical Journal International*, 219(2), pp.1138-1147.

967 Hizzett, J.L., Hughes Clarke, J.E., Sumner, E.J., Cartigny, M.J.B., Talling, P.J. and Clare, M.A., 2018.
968 Which triggers produce the most erosive, frequent, and longest runout turbidity currents on
969 deltas?. *Geophysical Research Letters*, 45(2), pp.855-863.

970 Howe, B.M., Arbic, B.K., Aucan, J., Barnes, C.R., Bayliff, N., Becker, N., Butler, R., Doyle, L., Elipot,
971 S., Johnson, G.C. and Landerer, F., 2019. SMART cables for observing the global ocean: science and
972 implementation. *Frontiers in Marine Science*, 6, p.424.

973 Hughes Clarke, J.E, Brucker, S., Muggah, J., Church, I., Cartwright, D., Kuus, P., Hamilton, T., Pratomo,
974 D. and Eisan, B., 2012. The Squamish ProDelta: monitoring active landslides and turbidity currents.
975 In *Canadian Hydrographic Conference 2012, Proceedings* (p. 15).

976 Hunt, J.E., Tappin, D.R., Watt, S.F.L., Susilohadi, S., Novellino, A, Ebmeier, S.K, Cassidy, M., Engwell,
977 S.L., Grilli, S.T., Hanif, M., Priyanto, W.S., Clare, M.A., Abdurrachman, M., Udrek, U. 2021. (In
978 Press). Submarine landslide megablocks show half of Anak Krakatau island failed on December 22nd,
979 2018, *Nature Communications*.

980 Iannucci, R., Lenti, L. and Martino, S., 2020. Seismic monitoring system for landslide hazard assessment
981 and risk management at the drainage plant of the Peschiera Springs (Central Italy). *Engineering*
982 *Geology*, 277, p.105787.

983 Ide, S., Araki, E. and Matsumoto, H., 2021. Very broadband strain-rate measurements along a submarine
984 fiber-optic cable off Cape Muroto, Nankai subduction zone, Japan. *Earth, Planets and Space*, 73(1),
985 pp.1-10.

986 Inman, D.L., Nordstrom, C.E. and Flick, R.E., 1976. Currents in submarine canyons: An air-sea-land
987 interaction. *Annual Review of Fluid Mechanics*, 8(1), pp.275-310.

988 Jeffreys, H., 1923. The Pamir Earthquake of 1911 February 18, in Relation to the Depths of Earthquake
989 Foci. *Geophysical Journal International*, 1, pp.22-31.

990 Kanamori, H. and Given, J.W., 1982. Analysis of long-period seismic waves excited by the May 18,
991 1980, eruption of Mount St. Helens—A terrestrial monopole?. *Journal of Geophysical Research: Solid*
992 *Earth*, 87(B7), pp.5422-5432.

993 Kawakatsu, H., 1989. Centroid single force inversion of seismic waves generated by landslides. *Journal*
994 *of Geophysical Research: Solid Earth*, 94(B9), pp.12363-12374.

995 Kelner, M., Migeon, S., Tric, E., Couboulex, F., Dano, A., Lebourg, T., & Taboada, A. (2016). Frequency
996 and triggering of small-scale submarine landslides on decadal timescales: Analysis of 4D bathymetric
997 data from the continental slope offshore Nice (France). *Marine Geology*, 379, 281-297.

998 Khripounoff, A., Vangriesheim, A., Babonneau, N., Crassous, P., Dennielou, B. and Savoye, B., 2003.
999 Direct observation of intense turbidity current activity in the Zaire submarine valley at 4000 m water
1000 depth. *Marine Geology*, 194(3-4), pp.151-158.

1001 Khripounoff, A., Crassous, P., Bue, N.L., Dennielou, B. and Jacinto, R.S., 2012. Different types of
1002 sediment gravity flows detected in the Var submarine canyon (northwestern Mediterranean
1003 Sea). *Progress in Oceanography*, 106, pp.138-153.

1004 Kioka, A., Schwestermann, T., Moernaut, J., Ikehara, K., Kanamatsu, T., McHugh, C.M., dos Santos
1005 Ferreira, C., Wiemer, G., Haghipour, N., Kopf, A.J. and Eglinton, T.I., 2019. Megathrust earthquake
1006 drives drastic organic carbon supply to the hadal trench. *Scientific reports*, 9(1), pp.1-10

- 1007 Lacroix, P., Grasso, J.R., Roulle, J., Giraud, G., Goetz, D., Morin, S. and Helmstetter, A., 2012.
1008 Monitoring of snow avalanches using a seismic array: Location, speed estimation, and relationships to
1009 meteorological variables. *Journal of Geophysical Research: Earth Surface*, 117(F1).
- 1010 Lecocq, T., Hicks, S.P., Van Noten, K., Van Wijk, K., Koelemeijer, P., De Plaen, R.S., Massin, F.,
1011 Hillers, G., Anthony, R.E., Apoloner, M.T. and Arroyo-Solórzano, M., 2020. Global quieting of high-
1012 frequency seismic noise due to COVID-19 pandemic lockdown measures. *Science*, 369(6509),
1013 pp.1338-1343.
- 1014 Leung, A.K. and Ng, C.W.W., 2016. Field investigation of deformation characteristics and stress
1015 mobilisation of a soil slope. *Landslides*, 13(2), pp.229-240.
- 1016 Lin, C.H., 2015. Insight into landslide kinematics from a broadband seismic network. *Earth, planets and*
1017 *space*, 67(1), p.8.
- 1018 Lin, C.H., Kumagai, H., Ando, M. and Shin, T.C., 2010. Detection of landslides and submarine slumps
1019 using broadband seismic networks. *Geophysical Research Letters*, 37(22).
- 1020 Lindsey, N.J. and Martin, E.R., 2021. Fiber-Optic Seismology. *Annual Review of Earth and Planetary*
1021 *Sciences*, 49, pp.309-336.+
- 1022 Lindsey, N.J., Dawe, T.C. and Ajo-Franklin, J.B., 2019. Illuminating seafloor faults and ocean dynamics
1023 with dark fiber distributed acoustic sensing. *Science*, 366(6469), pp.1103-1107.
- 1024
1025 Lintern, D. G., & Hill, P. R. (2010). An underwater laboratory at the Fraser River delta. *Eos, Transactions*
1026 *American Geophysical Union*, 91(38), 333-334.
- 1027 Lintern, D. G., Hill, P. R., & Stacey, C. (2016). Powerful unconfined turbidity current captured by cabled
1028 observatory on the Fraser River delta slope, British Columbia, Canada. *Sedimentology*.
- 1029 Lintern, D.G., Mosher, D.C. and Scherwath, M., 2019. Advancing from subaqueous mass movement case
1030 studies to providing advice and mitigation. *Geological Society, London, Special Publications*, 477, 1-
1031 14, 21 June 2019, <https://doi.org/10.1144/SP477-2018-190>
- 1032 Lior, I., Sladen, A., Rivet, D., Ampuero, J.P., Hello, Y., Becerril, C., Martins, H.F., Lamare, P., Jestin, C.,
1033 Tsagkli, S. and Markou, C., 2021. On the Detection Capabilities of Underwater Distributed Acoustic
1034 Sensing. *Journal of Geophysical Research: Solid Earth*, 126(3), p.e2020JB020925.

- 1035 Løvholt, F., Pedersen, G., Harbitz, C.B., Glimsdal, S. and Kim, J., 2015. On the characteristics of
1036 landslide tsunamis. *Philosophical Transactions of the Royal Society A: Mathematical, Physical and*
1037 *Engineering Sciences*, 373(2053), p.20140376.
- 1038 Mainsant, G., Larose, E., Brönnimann, C., Jongmans, D., Michoud, C. and Jaboyedoff, M., 2012.
1039 Ambient seismic noise monitoring of a clay landslide: Toward failure prediction. *Journal of*
1040 *Geophysical Research: Earth Surface*, 117(F1).
- 1041 Marra, G., Clivati, C., Lockett, R., Tampellini, A., Kronjäger, J., Wright, L., Mura, A., Levi, F.,
1042 Robinson, S., Xuereb, A. and Baptie, B., 2018. Ultrastable laser interferometry for earthquake
1043 detection with terrestrial and submarine cables. *Science*, 361(6401), pp.486-490.
- 1044 Maslin, M., Owen, M., Day, S. and Long, D., 2004. Linking continental-slope failures and climate
1045 change: Testing the clathrate gun hypothesis. *Geology*, 32(1), pp.53-56.
- 1046 Masson, D.G., Harbitz, C.B., Wynn, R.B., Pedersen, G. and Løvholt, F., 2006. Submarine landslides:
1047 processes, triggers and hazard prediction. *Philosophical Transactions of the Royal Society A:*
1048 *Mathematical, Physical and Engineering Sciences*, 364(1845), pp.2009-2039.
- 1049 Mastbergen, D., van den Ham, G., Cartigny, M., Koelewijn, A., de Kleine, M., Clare, M., ... & Vellinga,
1050 A. (2016). Multiple flow slide experiment in the Westerschelde Estuary, The Netherlands. In
1051 *Submarine Mass Movements and their Consequences* (pp. 241-249). Springer International
1052 Publishing.
- 1053 Matias, L.M., Carrilho, F., Sá, V., Omira, R., Niehus, M., Corela, C., Barros, J. and Omar, Y., 2021. The
1054 contribution of submarine optical fiber telecom cables to the monitoring of earthquakes and tsunamis
1055 in the NE Atlantic. *Frontiers in Earth Science*, 9, p.611.
- 1056 McAdoo, B.G., Pratson, L.F. and Orange, D.L., 2000. Submarine landslide geomorphology, US
1057 continental slope. *Marine Geology*, 169(1-2), pp.103-136.
- 1058 Mecozzi, A., Cantono, M., Castellanos, J.C., Kamalov, V., Muller, R. and Zhan, Z., 2021. Polarization
1059 sensing using submarine optical cables. *Optica*, 8(6), pp.788-795.
- 1060 Michlmayr, G., Chalari, A., Clarke, A. and Or, D., 2017. Fiber-optic high-resolution acoustic emission
1061 (AE) monitoring of slope failure. *Landslides*, 14(3), pp.1139-1146.

- 1062 Miramontes, E., Garziglia, S., Sultan, N., Jouet, G. and Cattaneo, A., 2018. Morphological control of
1063 slope instability in contourites: a geotechnical approach. *Landslides*, 15(6), pp.1085-1095.
- 1064 Mizutani, A., Yomogida, K. and Tanioka, Y., 2020. Early tsunami detection with near-fault ocean-bottom
1065 pressure gauge records based on the comparison with seismic data. *Journal of Geophysical Research:
1066 Oceans*, 125(9), p.e2020JC016275.
- 1067 Moernaut, J. and De Batist, M., 2011. Frontal emplacement and mobility of sublacustrine landslides:
1068 results from morphometric and seismostratigraphic analysis. *Marine Geology*, 285(1-4), pp.29-45.
- 1069 Mohrig, D. and Marr, J.G., 2003. Constraining the efficiency of turbidity current generation from
1070 submarine debris flows and slides using laboratory experiments. *Marine and Petroleum
1071 Geology*, 20(6-8), pp.883-899.
- 1072
- 1073 Moore, J.G., Clague, D.A., Holcomb, R.T., Lipman, P.W., Normark, W.R. and Torresan, M.E., 1989.
1074 Prodigious submarine landslides on the Hawaiian Ridge. *Journal of Geophysical Research: Solid
1075 Earth*, 94(B12), pp.17465-17484.
- 1076 Moretti, L., Allstadt, K., Mangeney, A., Capdeville, Y., Stutzmann, E. and Bouchut, F., 2015. Numerical
1077 modeling of the Mount Meager landslide constrained by its force history derived from seismic
1078 data. *Journal of Geophysical Research: Solid Earth*, 120(4), pp.2579-2599.
- 1079 Mountjoy, J.J., McKean, J., Barnes, P.M. and Pettinga, J.R., 2009. Terrestrial-style slow-moving
1080 earthflow kinematics in a submarine landslide complex. *Marine geology*, 267(3-4), pp.114-127.
- 1081 Mountjoy, J.J., Howarth, J.D., Orpin, A.R., Barnes, P.M., Bowden, D.A., Rowden, A.A., Schimel, A.C.,
1082 Holden, C., Horgan, H.J., Nodder, S.D. and Patton, J.R., 2018. Earthquakes drive large-scale
1083 submarine canyon development and sediment supply to deep-ocean basins. *Science advances*, 4(3),
1084 p.eaar3748.
- 1085 Mulder, T. and Cochonat, P., 1996. Classification of offshore mass movements. *Journal of Sedimentary
1086 research*, 66(1), pp.43-57.
- 1087 Nisbet, E.G. and Piper, D.J., 1998. Giant submarine landslides. *Nature*, 392(6674), pp.329-330.

1088 Nishimura, T., Emoto, K., Nakahara, H., Miura, S., Yamamoto, M., Sugimura, S., Ishikawa, A. and
1089 Kimura, T., 2021. Source location of volcanic earthquakes and subsurface characterization using fiber-
1090 optic cable and distributed acoustic sensing system. *Scientific reports*, 11(1), pp.1-12.

1091 Normandeau, A., Campbell, D.C., Piper, D.J. and Jenner, K.A., 2019. Are submarine landslides an
1092 underestimated hazard on the western North Atlantic passive margin?. *Geology*, 47(9), pp.848-852.

1093 Normandeau, A., MacKillop, K., Macquarrie, M., Richards, C., Bourgault, D., Campbell, D.C., Maselli,
1094 V., Philibert, G. and Clarke, J.H., 2021. Submarine landslides triggered by iceberg collision with the
1095 seafloor. *Nature Geoscience*, 14(8), pp.599-605.

1096 Nwoko, J., Kane, I. and Huuse, M., 2020. Megaclasts within mass-transport deposits: their origin,
1097 characteristics and effect on substrates and succeeding flows. *Geological Society, London, Special
1098 Publications*, 500(1), pp.515-530.

1099 Obelcz, J., Xu, K., Georgiou, I.Y., Maloney, J., Bentley, S.J. and Miner, M.D., 2017. Sub-decadal
1100 submarine landslides are important drivers of deltaic sediment flux: Insights from the Mississippi
1101 River Delta Front. *Geology*, 45(8), pp.703-706.

1102 Obelcz, J., Wood, W.T., Phrampus, B.J. and Lee, T.R., 2020. Machine learning augmented time-lapse
1103 bathymetric surveys: A case study from the Mississippi river delta front. *Geophysical Research
1104 Letters*, 47(10), p.e2020GL087857.

1105 Ogata, K., Festa, A. and Pini, G.A. eds., 2019. *Submarine Landslides: Subaqueous Mass Transport
1106 Deposits from Outcrops to Seismic Profiles* (Vol. 247). John Wiley & Sons.

1107 Parker, G., 1982. Conditions for the ignition of catastrophically erosive turbidity currents. *Marine
1108 Geology*, 46(3-4), pp.307-327.

1109 Paull, C.K., Talling, P.J., Maier, K.L., Parsons, D., Xu, J., Caress, D.W., Gwiazda, R., Lundsten, E.M.,
1110 Anderson, K., Barry, J.P. and Chaffey, M., 2018. Powerful turbidity currents driven by dense basal
1111 layers. *Nature communications*, 9(1), pp.1-9.

1112 Paull, C.K., Ussler, W. and Holbrook, W.S., 2007. Assessing methane release from the colossal Storegga
1113 submarine landslide. *Geophysical research letters*, 34(4).

1114 Piper, D.J., Cochonat, P. and Morrison, M.L., 1999. The sequence of events around the epicentre of the
1115 1929 Grand Banks earthquake: initiation of debris flows and turbidity current inferred from sidescan
1116 sonar. *Sedimentology*, 46(1), pp.79-97.

1117 Pope, E.L., Talling, P.J., Carter, L., Clare, M.A. and Hunt, J.E., 2017. Damaging sediment density flows
1118 triggered by tropical cyclones. *Earth and Planetary Science Letters*, 458, pp.161-169.

1119 Puzrin, A.M., Germanovich, L.N. and Friedli, B., 2016. Shear band propagation analysis of submarine
1120 slope stability. *Géotechnique*, 66(3), pp.188-201.

1121 Prior, D.B., Bornhold, B.D., Coleman, J.M. and Bryant, W.R., 1982. Morphology of a submarine slide,
1122 Kitimat arm, British Columbia. *Geology*, 10(11), pp.588-592.

1123 Prior, D.B., Suhayda, J.N., Lu, N.Z., Bornhold, B.D., Keller, G.H., Wiseman, W.J., Wright, L.D. and
1124 Yang, Z.S., 1989. Storm wave reactivation of a submarine landslide. *Nature*, 341(6237), pp.47-50

1125 Puzrin, A.M., Germanovich, L.N. and Friedli, B., 2016. Shear band propagation analysis of submarine
1126 slope stability. *Géotechnique*, 66(3), pp.188-201.

1127 Ranasinghe, N., Rowe, C., Syracuse, E., Larmat, C. and Begnaud, M., 2018. Enhanced global seismic
1128 resolution using transoceanic SMART cables. *Seismological Research Letters*, 89(1), pp.77-85.

1129 Rickenmann, D., 2017. Bedload transport measurements with geophones, hydrophones and underwater
1130 microphones (passive acoustic methods). *Gravel Bed Rivers and Disasters*, Wiley & Sons, Chichester,
1131 UK, pp.185-208.

1132 Roche, B., Bull, J.M., Marin-Moreno, H., Leighton, T.G., Falcon-Suarez, I.H., Tholen, M., White, P.R.,
1133 Provenzano, G., Lichtschlag, A., Li, J. and Faggetter, M., 2021. Time-lapse imaging of CO2 migration
1134 within near-surface sediments during a controlled sub-seabed release experiment. *International*
1135 *Journal of Greenhouse Gas Control*, 109, p.103363.

1136 Rouse, C., Styles, P. and Wilson, S.A., 1991. Microseismic emissions from flowslide-type movements in
1137 South Wales. *Engineering Geology*, 31(1), pp.91-110.

1138 Ryan, J.P., Joseph, J.E., Margolina, T., Peavey Reeves, L., Hatch, L., DeVogelaere, A., Southall, B.,
1139 Stimpert, A. and Baumann-Pickering, S., 2020. Quieting of low-frequency vessel noise in Monterey
1140 Bay National Marine Sanctuary during the COVID-19 pandemic. *The Journal of the Acoustical*
1141 *Society of America*, 148(4), pp.2734-2734.

1142 Sammartini, M., Moernaut, J., Kopf, A., Stegmann, S., Fabbri, S.C., Anselmetti, F.S. and Strasser, M.,
1143 2021. Propagation of frontally confined subaqueous landslides: Insights from combining geophysical,
1144 sedimentological, and geotechnical analysis. *Sedimentary Geology*, p.105877.

1145 Sgroi, T., Monna, S., Embriaco, D., Giovanetti, G., Marinaro, G. and Favali, P., 2014. Geohazards in the
1146 western Ionian Sea: Insights from non-earthquake signals recorded by the NEMO-SN1 seafloor
1147 observatory. *Oceanography*, 27(2), pp.154-166.

1148 Simmons, S.M., Azpiroz-Zabala, M., Cartigny, M.J.B., Clare, M.A., Cooper, C., Parsons, D.R., Pope,
1149 E.L., Sumner, E.J. and Talling, P.J., 2020. Novel acoustic method provides first detailed
1150 measurements of sediment concentration structure within submarine turbidity currents. *Journal of*
1151 *Geophysical Research: Oceans*, 125(5), p.e2019JC015904.

1152 Smith, D.P., Kvittek, R., Iampietro, P.J. and Wong, K., 2007. Twenty-nine months of geomorphic change
1153 in upper Monterey Canyon (2002–2005). *Marine Geology*, 236(1-2), pp.79-94.

1154 Stegmann, S., Sultan, N., Kopf, A., Apprioual, R., & Pelleau, P. (2011). Hydrogeology and its effect on
1155 slope stability along the coastal aquifer of Nice, France. *Marine Geology*, 280(1), 168-181.

1156 Strasser, M., Kölling, M., Ferreira, C.D.S., Fink, H.G., Fujiwara, T., Henkel, S., Ikehara, K., Kanamatsu,
1157 T., Kawamura, K., Kodaira, S. and Römer, M., 2013. A slump in the trench: Tracking the impact of
1158 the 2011 Tohoku-Oki earthquake. *Geology*, 41(8), pp.935-938.

1159 Strout, J. M., & Tjelta, T. I. (2005). In situ pore pressures: What is their significance and how can they be
1160 reliably measured?. *Marine and Petroleum Geology*, 22(1), 275-285.

1161 Sukhovich, A., Bonnieux, S., Hello, Y., Irissou, J.O., Simons, F.J. and Nolet, G., 2015. Seismic
1162 monitoring in the oceans by autonomous floats. *Nature communications*, 6(1), pp.1-6.

1163 Sultan, N., Savoye, B., Jouet, G., Leynaud, D., Cochonat, P., Henry, P., Stegmann, S. and Kopf, A., 2010.
1164 Investigation of a possible submarine landslide at the Var delta front (Nice continental slope, southeast
1165 France). *Canadian Geotechnical Journal*, 47(4), pp.486-496.

1166 Sumner, E.J. and Paull, C.K., 2014. Swept away by a turbidity current in Mendocino submarine canyon,
1167 California. *Geophysical Research Letters*, 41(21), pp.7611-7618.

1168 Suriñach, E., Vilajosana, I., Khazaradze, G., Biescas, B., Furdada, G. and Vilaplana, J.M., 2005. Seismic
1169 detection and characterization of landslides and other mass movements. *Natural Hazards and Earth*
1170 *System Sciences*, 5(6), pp.791-798.

1171 Talling, P.J., Paull, C.K. and Piper, D.J., 2013. How are subaqueous sediment density flows triggered,
1172 what is their internal structure and how does it evolve? Direct observations from monitoring of active
1173 flows. *Earth-Science Reviews*, 125, pp.244-287.

1174 Talling, P.J., Wynn, R.B., Masson, D.G., Frenz, M., Cronin, B.T., Schiebel, R., Akhmetzhanov, A.M.,
1175 Dallmeier-Tiessen, S., Benetti, S., Weaver, P.P.E. and Georgiopoulou, A., 2007. Onset of submarine
1176 debris flow deposition far from original giant landslide. *Nature*, 450(7169), pp.541-544.

1177 Tappin, D.R., Grilli, S.T., Harris, J.C., Geller, R.J., Masterlark, T., Kirby, J.T., Shi, F., Ma, G.,
1178 Thingbaijam, K.K.S. and Mai, P.M., 2014. Did a submarine landslide contribute to the 2011 Tohoku
1179 tsunami?. *Marine Geology*, 357, pp.344-361.

1180 Tappin, D.R., Watts, P. and Grilli, S.T., 2008. The Papua New Guinea tsunami of 17 July 1998: anatomy
1181 of a catastrophic event. *Natural Hazards and Earth System Sciences*, 8(2), pp.243-266.

1182 Ten Brink, U.S., Geist, E.L. and Andrews, B.D., 2006. Size distribution of submarine landslides and its
1183 implication to tsunami hazard in Puerto Rico. *Geophysical Research Letters*, 33(11).

1184 Ten Brink, U., Twichell, D., Geist, E., Chaytor, J., Locat, J., Lee, H., Buczkowski, B., Barkan, R., Solow,
1185 A., & Andrews, B. (2008). Evaluation of tsunami sources with the potential to impact the US Atlantic
1186 and Gulf coasts, U.S. Geological Survey Administrative report to the US Nuclear Regulatory
1187 Commission 300.

1188 Thirugnanam, H., Ramesh, M.V. and Rangan, V.P., 2020. Enhancing the reliability of landslide early
1189 warning systems by machine learning. *Landslides*, 17(9), pp.2231-2246.

1190 Urgeles, R. and Camerlenghi, A., 2013. Submarine landslides of the Mediterranean Sea: Trigger
1191 mechanisms, dynamics, and frequency-magnitude distribution. *Journal of Geophysical Research:*
1192 *Earth Surface*, 118(4), pp.2600-2618.

1193 Urlaub, M., Petersen, F., Gross, F., Bonforte, A., Puglisi, G., Guglielmino, F., Krastel, S., Lange, D. and
1194 Kopp, H., 2018. Gravitational collapse of Mount Etna's southeastern flank. *Science Advances*, 4(10),
1195 p.eaat9700.

1196 Urlaub, M., Talling, P.J. and Masson, D.G., 2013. Timing and frequency of large submarine landslides:
1197 implications for understanding triggers and future geohazard. *Quaternary Science Reviews*, 72, pp.63-
1198 82.

1199 Urlaub, M., Talling, P.J. and Clare, M., 2014. Sea-level-induced seismicity and submarine landslide
1200 occurrence: Comment. *Geology*, 42(6), pp.e337-e337.

1201 Urlaub, M. and Villinger, H., 2019. Combining in situ monitoring using seabed instruments and
1202 numerical modelling to assess the transient stability of underwater slopes. *Geological Society, London,*
1203 *Special Publications*, 477(1), pp.511-521.

1204 Vanneste, M., Sultan, N., Garziglia, S., Forsberg, C. F., & L'Heureux, J. S. (2014). Seafloor instabilities
1205 and sediment deformation processes: the need for integrated, multi-disciplinary investigations. *Marine*
1206 *Geology*, 352, 183-214.

1207 Van Herwijnen, A., Heck, M. and Schweizer, J., 2016. Forecasting snow avalanches using avalanche
1208 activity data obtained through seismic monitoring. *Cold Regions Science and Technology*, 132, pp.68-
1209 80.

1210 Van Herwijnen, A. and Schweizer, J., 2011. Seismic sensor array for monitoring an avalanche start zone:
1211 design, deployment and preliminary results. *Journal of Glaciology*, 57(202), pp.267-276.

1212 Vardy, M.E., L'Heureux, J.S., Vanneste, M., Longva, O., Steiner, A., Forsberg, C.F., Haflidason, H. and
1213 Brendryen, J., 2012. Multidisciplinary investigation of a shallow near-shore landslide, Finneidfjord,
1214 Norway. *Near Surface Geophysics*, 10(4), pp.267-277.

1215 Waage, M., Singhroha, S., Bünz, S., Planke, S., Waghorn, K.A. and Bellwald, B., 2021. Feasibility of
1216 using the P-Cable high-resolution 3D seismic system in detecting and monitoring CO2
1217 leakage. *International Journal of Greenhouse Gas Control*, 106, p.103240.

1218 Walter, T.R., Haghghi, M.H., Schneider, F.M., Coppola, D., Motagh, M., Saul, J., Babeyko, A., Dahm,
1219 T., Troll, V.R., Tilmann, F. and Heimann, S., 2019. Complex hazard cascade culminating in the Anak
1220 Krakatau sector collapse. *Nature communications*, 10(1), pp.1-11.

1221 Wilcock, W., 2021. Illuminating tremors in the deep. *Science*, 371(6532), pp.882-884.

- 1222 Williams, E.F., Fernández-Ruiz, M.R., Magalhaes, R., Vanthillo, R., Zhan, Z., González-Herráez, M. and
1223 Martins, H.F., 2019. Distributed sensing of microseisms and teleseisms with submarine dark
1224 fibers. *Nature communications*, 10(1), pp.1-11.
- 1225 Xu, J.P., 2010. Normalized velocity profiles of field-measured turbidity currents. *Geology*, 38(6), pp.563-
1226 566.
- 1227 Xu, J.P., 2011. Measuring currents in submarine canyons: Technological and scientific progress in the
1228 past 30 years. *Geosphere*, 7(4), pp.868-876.
- 1229 Yamada, M., Kumagai, H., Matsushi, Y. and Matsuzawa, T., 2013. Dynamic landslide processes revealed
1230 by broadband seismic records. *Geophysical Research Letters*, 40(12), pp.2998-3002.
- 1231 Ye, L., Kanamori, H., Rivera, L., Lay, T., Zhou, Y., Sianipar, D. and Satake, K., 2020. The 22 December
1232 2018 tsunami from flank collapse of Anak Krakatau volcano during eruption. *Science advances*, 6(3),
1233 p.eaaz1377.
- 1234 Yeh, Y.C., Tsai, C.L., Hsu, S.K., Lin, H.S., Chen, K.T., Cho, Y.Y. and Liang, C.W., 2021. Continental
1235 shelf morphology controlled by bottom currents, mud diapirism, and submarine slumping to the east
1236 of the Gaoping Canyon, off SW Taiwan. *Geo-Marine Letters*, 41(1), pp.1-11.
- 1237 Yuan, X., Kind, R. and Pedersen, H.A., 2005. Seismic monitoring of the Indian Ocean
1238 tsunami. *Geophysical research letters*, 32(15).
- 1239 Zeng, J., Lowe, D.R., Prior, D.B., Wiseman JR, W.J. and Bornhold, B.D., 1991. Flow properties of
1240 turbidity currents in Bute Inlet, British Columbia. *Sedimentology*, 38(6), pp.975-996.
- 1241 Zhan, Z., 2020. Distributed acoustic sensing turns fiber-optic cables into sensitive seismic
1242 antennas. *Seismological Research Letters*, 91(1), pp.1-15.
- 1243 Zhan, Z., Cantono, M., Kamalov, V., Mecozzi, A., Müller, R., Yin, S. and Castellanos, J.C., 2021.
1244 Optical polarization-based seismic and water wave sensing on transoceanic
1245 cables. *Science*, 371(6532), pp.931-936.
- 1246 Zhang, Y., Liu, Z., Zhao, Y., Colin, C., Zhang, X., Wang, M., Zhao, S. and Kneller, B., 2018. Long-term
1247 in situ observations on typhoon-triggered turbidity currents in the deep sea. *Geology*, 46(8), pp.675-
1248 678.

1249 Zhao, S., Wang, Z., Nie, Z., He, K. and Ding, N., 2021. Investigation on total adjustment of the
1250 transducer and seafloor transponder for GNSS/Acoustic precise underwater point positioning. *Ocean*
1251 *Engineering*, 221, p.108533.
1252